Volume 43 | Number 36 | 28 September 2014 | Pages 13447–13816

Dalton Transactions

An international journal of inorganic chemistry

www.rsc.org/dalton

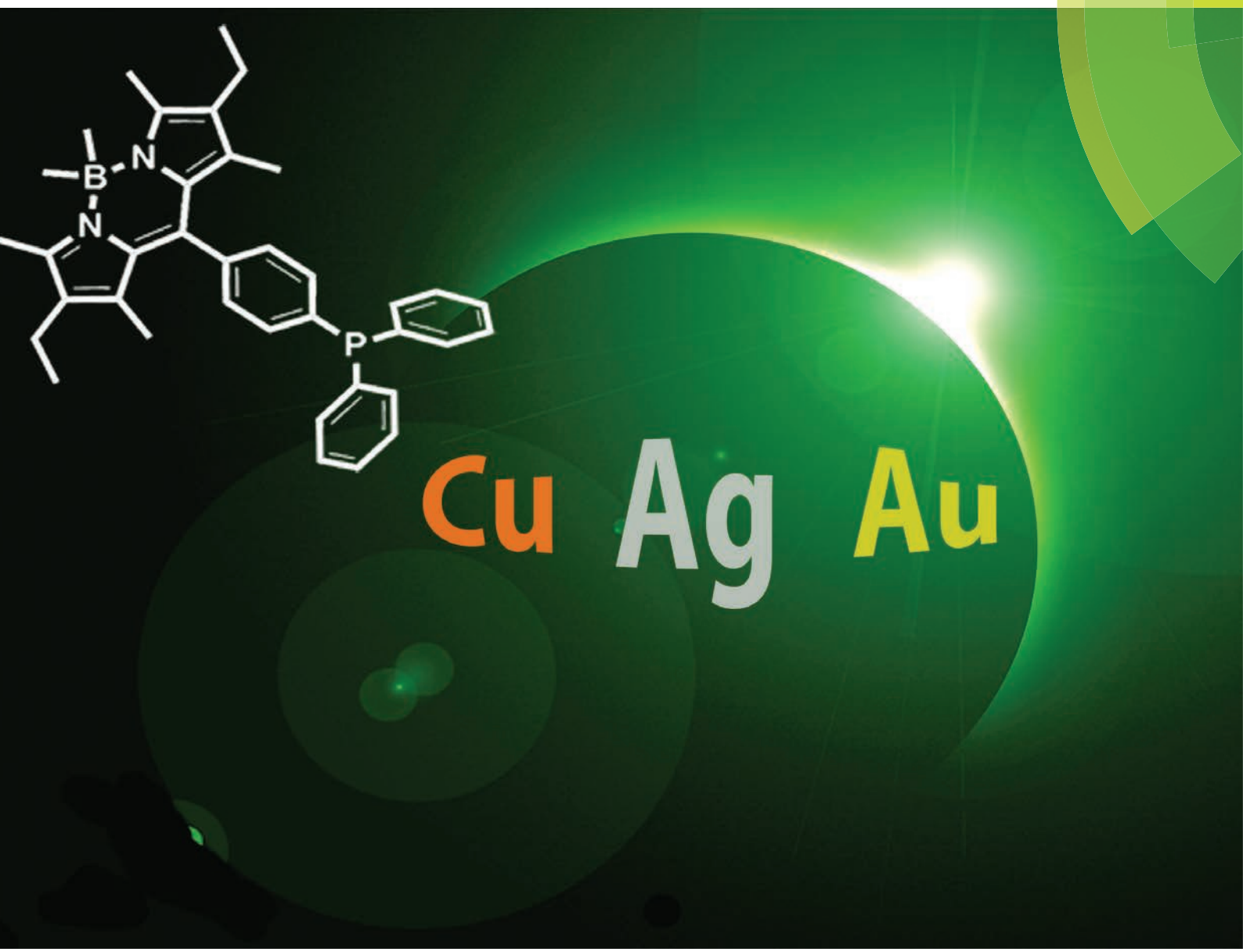

ISSN 1477-9226

ROYAL SOCIETY OF CHEMISTRY

PAPER

Lee J. Higham *et al.*

$^{B}R_2BodPR_2$: highly fluorescent alternatives to PPh_3 and $PhPCy_2$

Dalton Transactions

PAPER

View Article Online
View Journal | View Issue

Cite this: *Dalton Trans.*, 2014, **43**, 13485

$^{B}R_2BodPR_2$: highly fluorescent alternatives to PPh_3 and $PhPCy_2$†

Laura H. Davies, Ross W. Harrington, William Clegg and Lee J. Higham*

Received 8th March 2014,
Accepted 27th May 2014

DOI: 10.1039/c4dt00704b

www.rsc.org/dalton

The syntheses of highly fluorescent analogues of PPh_3 and $PhPCy_2$ based on the Bodipy chromophore are described. The ligands have been incorporated into two- to four-coordinate group 11 metal complexes. The synthesis, characterisation and photophysical properties of the novel ligands and their metal complexes are reported; many of these compounds have also been characterised by single-crystal X-ray diffraction. Incorporation of the phosphino group and complexation to the group 11 metal centre has little effect on the absorption and emission profiles; high molar extinction coefficients and fluorescence quantum yields were still obtained. In particular, incorporation of the dicyclohexylphosphino substituent significantly increases the quantum yields relative to the parent dyes.

Introduction

Metal complexes of fluorescent phosphines have potential applications in diagnostic cell imaging[1] and catalytic reaction monitoring,[2] by virtue of the sensitivity of the fluorescence technique. As an imaging tool used *in vitro*, fluorescence microscopy produces high spatial resolution of the nanometre order, giving accurate images of processes at the subcellular level;[1,3] there is current interest in incorporating fluorescent tags onto radiopharmaceuticals, because it is otherwise difficult to image the localisation of such probes in detail. A fluorescent radiopharmaceutical would instead facilitate both *in vivo* and *in vitro* imaging,[3] allowing one to gain a better understanding of the probe's mechanism and localisation within cells. The sensitivity of fluorescence spectroscopy compared to its NMR counterpart (10^{-6} to 10^{-7} M), also signifies that the detection of low concentrations of catalytically active species – undetectable by other means – ought to also be possible.[2] However, phosphines conjugated to organic fluorophores often suffer from fluorescence quenching[4] due to reductive photoinduced electron transfer, therefore synthetic routes to this class of compound have not been extensively reported and fluorescent phosphines remain somewhat rare.[5]

F-Bodipy has desirable photophysical properties which include a high fluorescence quantum yield, strong UV-absorption, chemical robustness and good solubility (Fig. 1).[6] A common site of modification is at the *meso* position due to its easy synthetic incorporation.[6] Over the last few years new synthetic procedures have been developed for the substitution of the fluorides with aryl/alkyl (*C*-Bodipy) or ethynyl (*E*-Bodipy) groups; this development has allowed more sophisticated functions to be introduced on the Bodipy backbone.[6] Given the desirable properties of Bodipy and the extensive synthetic routes to derivatives,[6] we aimed to create fluorescent tertiary phosphines based on this versatile fluorophore, coordinate the new ligands to transition metals and study their behaviour.

Group 11 metal phosphine complexes are sought after, in part, due to their known medicinal applications.[7] Gold(I),[8] silver(I)[9] and copper(I)[10] phosphine complexes have all shown cytotoxic activity, with significant anti-tumour properties – current complexes are based on monodentate and bidentate phosphines. One breakthrough was the discovery of auranofin (Fig. 1) in the early 1980s by Sutton,[11] a gold(I) phosphine complex, that was approved for clinical use in 1985 to treat rheumatoid arthritis, but which has also been shown to exhibit anticancer properties,[12] and led to the development of several two-coordinate gold(I) phosphine analogues.[8]

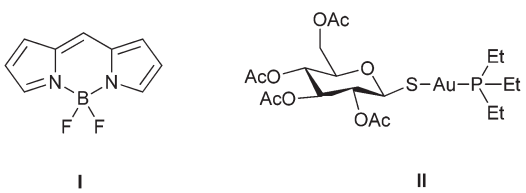

I II

Fig. 1 *F*-Bodipy (I) and auranofin (II).

School of Chemistry, Bedson Building, Newcastle University, Newcastle upon Tyne, NE1 7RU, UK. E-mail: lee.higham@ncl.ac.uk; Tel: +44 (0)191 208 5542

†Electronic supplementary information (ESI) available: Experimental methods, spectroscopic and crystallographic characterisation, photophysical measurements and molecular modelling details. CCDC 987389, 987388, 987387, 987386, 987385, 987390, 987384, 987391, 987383 and 987382. For ESI and crystallographic data in CIF or other electronic format see DOI: 10.1039/c4dt00704b

To further develop the possibility of using gold-based drugs, a greater knowledge of their subcellular distribution and mechanism of action is desirable – a fluorescent gold phosphine complex could help to understand the biodistribution of such compounds at high resolution and precision.[1,3] Both gold and silver also have potential in therapeutic nuclear medicine due to the beta-emitting radioisotopes ^{199}Au and ^{111}Ag, which have long half-lives of 3.15 and 7.5 days respectively.[13] Copper has a range of radionuclides, but the most commonly investigated is ^{64}Cu – a positron emitter – and thus can be used for diagnostic nuclear medicine purposes in Positron Emission Tomography (PET) imaging; its relatively long half-life of 762 minutes is considered attractive.[14] For the aforementioned reasons it would therefore be interesting to investigate the coordination chemistry of novel fluorescent monodentate phosphines with the group 11 metals and measure the photophysical properties of any complexes so synthesised, to ascertain if they are suitable for study in the applications already discussed above.

Results and discussion

Synthesis of Bodipy monodentate phosphines

Scheme 1 details our synthesis of the four novel Bodipy monodentate tertiary phosphines **2a**/**2b** and **3a**/**3b**, substituted at the *meso* position; aryl bromides **1a** and **1b**[15] were lithiated by reacting with *n*-butyllithium in diethyl ether at −78 °C to room temperature, followed by the addition of chlorodiphenylphosphine or chlorodicyclohexylphosphine. Both aryl- and alkylchlorophosphines reacted in a similar manner and we also found that the substituent at the boron atom had a limited effect on the overall reactivity of the aryl bromide; all four ligands were produced in good yields ranging from 60 to 84%. The route thus depicts a mild synthetic method for preparing phosphines containing a Bodipy fluorophore.

The ^{31}P{^{1}H} NMR spectra of the triarylphosphines in *d*-chloroform showed **2a**/**2b** at δ −5.5 ppm; aryldialkylphosphines **3a** and **3b** are shifted downfield to δ 2.7 and 2.8 ppm respectively, due to the electron-donating cyclohexyl rings.

Crystals of **2a** were analysed by X-ray crystallography and its molecular structure is depicted in Fig. 2; similar atom numbering schemes are used for all the crystal structures. The P–C bond lengths of 1.8302(19), 1.834(2) and 1.827(2) Å and C–P–C bond angles of 104.03(9), 101.66(9) and 102.40(9)° are typical for tertiary phosphines and compare well to triphenylphosphine.[16]

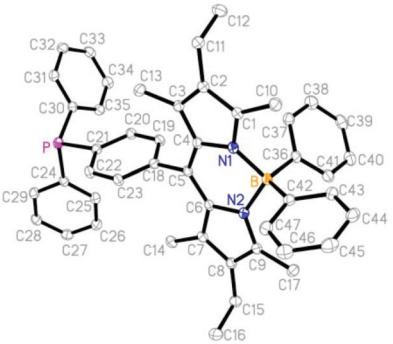

Fig. 2 Molecular structure of **2a** with 30% probability displacement ellipsoids (as in other figures). Hydrogen atoms have been omitted for clarity. Selected bond distances [Å] and angles [°]: P–C21 1.8302(19), P–C24 1.834(2), P–C30 1.827(2), C4–C5 1.395(3), N1–C4 1.400(2), N1–B 1.568(2), B–C36 1.626(3); C21–P–C24 101.66(9), C21–P–C30 104.03(9), C24–P–C30 102.40(9), C4–C5–C6 122.44(16), B–N1–C4 123.14(15), N1–B–C36 107.65(15), N1–B–N2 105.17(15).

Coordination chemistry

Copper. Tetrakis(acetonitrile)copper(I) hexafluorophosphate was treated with two equivalents of **2a**/**2b** or **3a**/**3b** in dichloromethane which led to the formation of [Cu(**2a**/**2b**)$_2$(CH$_3$CN)][PF$_6$] (**4a**/**4b**) and [Cu(**3a**/**3b**)$_2$(CH$_3$CN)][PF$_6$] (**5a**/**5b**), as depicted in Scheme 2; two phosphines coordinate to the copper(I) centre, replacing the labile acetonitrile ligands. Coordination of the phosphines causes a broadening and downfield shift of the ^{31}P{^{1}H} NMR signal from δ −5.5, and 2.7/2.8 ppm for the free phosphines **2a**/**2b** and **3a**/**3b** to δ 0.0/0.1, and 13.4/12.7 ppm for the complexes **4a**/**4b** and **5a**/**5b** respectively – these values compare well to other copper(I) acetonitrile phosphine complexes.[17,18] Crystals of **4a** and **4b** suitable for X-ray crystallography were obtained by slow diffusion from ethanol/pentane; the molecular structure of **4b** is depicted in Fig. 3, whilst the structure of a compound obtained from the attempted recrystallization of **4a** is given in the ESI.† Complex **4b** contains a three-coordinate copper(I) centre with a non-coordinating PF_6^- anion and one ethanol molecule, which has exchanged for the labile acetonitrile ligand, coordinated to the copper centre.

The Cu–P bond lengths of 2.2384(11) and 2.2273(11) Å are typical for copper(I) complexes.[18,19] The complex has a dis-

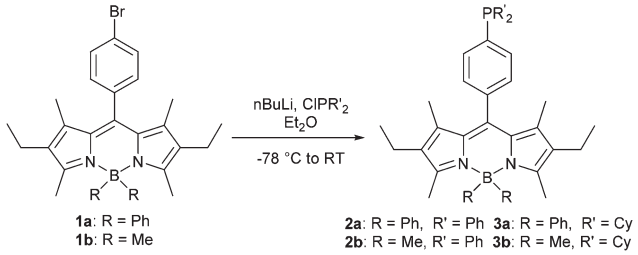

Scheme 1 Synthesis of the *C*-Bodipy substituted tertiary phosphine derivatives.

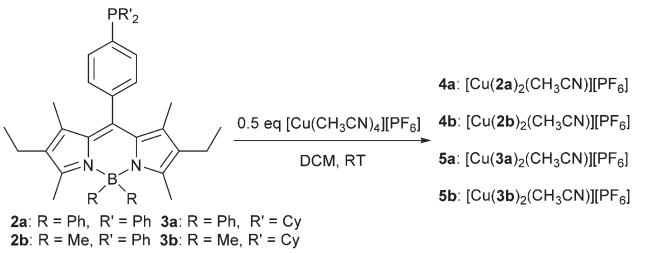

Scheme 2 Synthesis of copper(I) complexes **4a**/**4b** and **5a**/**5b**.

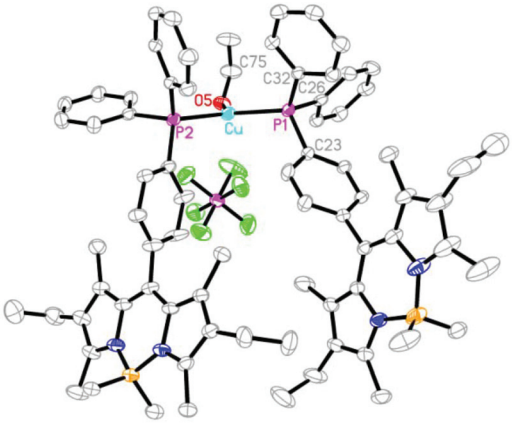

Fig. 3 View of the molecular structure of **4b** with selected atom labels. Hydrogen atoms bound to carbon have been omitted for clarity. Selected bond distances [Å] and angles [°]: Cu–P1 2.2384(11), Cu–P2 2.2273(11), Cu–O5 2.063(3), P1–C23 1.824(4), P1–C26 1.821(4), P1–C32 1.831(4), O5–C75 1.409(5); P1–Cu–P2 130.49(4), P1–Cu–O5 113.61(9), P2–Cu–O5 115.43(9).

torted trigonal planar geometry for copper, shown by the P1–Cu–P2, P1–Cu–O5 and P2–Cu–O5 bond angles of 130.49(4)°, 113.61(9)° and 115.43(9)° respectively; both the phosphorus atoms are slightly tilted towards the ethanol molecule. The anion···Cu(I) interaction is weak as signified by the closest Cu···F distance of 3.156 Å. The analogous reaction of a 2 : 1 ratio of triphenylphosphine and $[Cu(CH_3CN)_4][PF_6]$ resulted in the distorted four-coordinate tetrahedral complex $[Cu(PPh_3)_2(CH_3CN)_2]$.[17,20] Ligand **2b** is sterically more bulky than triphenylphosphine, and therefore the four-coordinate structure may be too crowded for the first-row d^{10} transition metal in this case.

Complex **5a** was crystallised by slow solvent diffusion (chloroform–diethyl ether); two types of crystals were produced and their molecular structures are shown in Fig. 4. Structure **A** is a three-coordinate copper(I) complex with two phosphines and one acetonitrile ligand coordinated to the copper centre, and a non-coordinating anion, PF_6^-. The Cu–P bond lengths of 2.2273(11) and 2.2564(10) Å are typical of copper(I) phosphine complexes.[18,19] The complex has a distorted trigonal planar geometry as shown by the P1–Cu–P2, P1–Cu–N5 and P2–Cu–N5 bond angles of 136.11(4)°, 120.68(10)° and 102.36(10)° respectively; the P1–Cu–P2 angle is larger than in complex **4b** due to the steric bulk of the cyclohexyl groups. The anion···Cu(I) interaction is again weak, as signified by the closest Cu···F distance of 3.228 Å. Structure **B** is a distorted trigonal-planar copper(I) complex with two phosphines coordinated and no bound acetonitrile ligands, but the PF_6^- anion (modelled with disorder) is weakly coordinated to the copper centre as shown by a stronger anion···Cu(I) interaction than in structure **A**; the alternative closest Cu···F distances are 2.741(7) Å to F6A as shown in Fig. 4, and 2.964(11) Å to F6B (not shown); F6A is disordered over two symmetry-related positions in the trigonal plane with the copper centre (on a twofold rotation axis) and two P atoms. All other Cu···F distances are

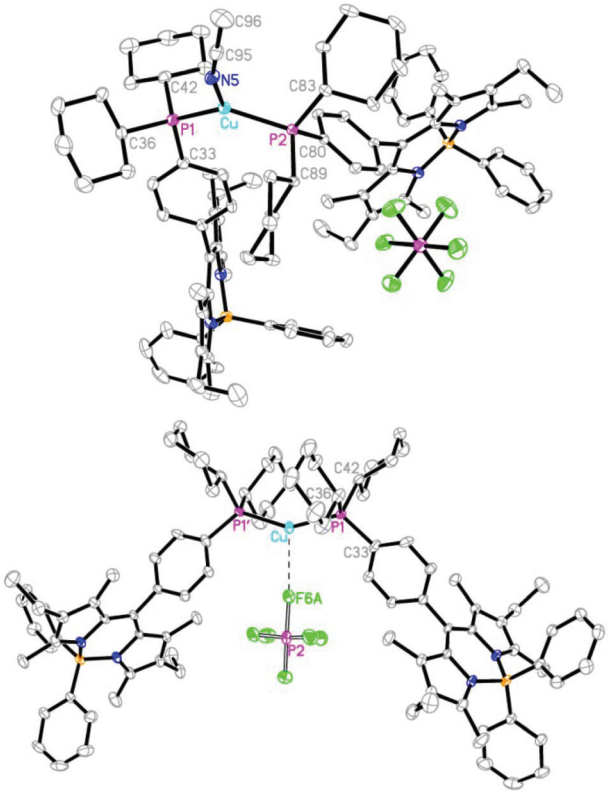

Fig. 4 View of the molecular structures of **5a** structure A (top) and **5a** structure B (bottom). Hydrogen atoms have been omitted for clarity. Selected bond distances [Å] and angles [°]: **5a** structure **A** – Cu–P1 2.2273(11), Cu–P2 2.2564(10), Cu–N5 1.994(3), P1–C33 1.829(4), P1–C42 1.841(4), P2–C83 1.845(4), N5–C95 1.128(5), C95–C96 1.466(6); P1–Cu–P2 136.11(4), P1–Cu–N5 120.68(10), P2–Cu–N5 102.36(10), C83–P2–C89 107.56(16), C80–P2–C83 101.98(15), Cu–P2–C83 110.59(12), Cu–P2–C80 122.24(12). **5a** structure **B** – Cu–P1 2.2280(15), P1–C33 1.819(4), P1–C36 1.866(5), P1–C42 1.867(5), Cu···F6A 2.741; P1–Cu–P1′ 149.98(9), Cu–P1–C33 121.92(17), Cu–P1–C36 111.55(16), C33–P1–C36 102.6(2).

>4 Å and are thus non-bonded. A search of the Cambridge Structural Database[21] reveals 11 structures recorded with weakly coordinated PF_6^- and BF_4^- anions having Cu···F > 2.7 Å.[22] The P–Cu–P bond angle of 149.98(9)° is large for a three-coordinate structure but is consistent with the steric bulk of the cyclohexyl groups and is similar to that in the three-coordinate complex $[Cu(PCy_3)_2(ClO_4)]$, which has a P–Cu–P angle of 144.46(6)°.[23] The symmetry-equivalent Cu–P bonds lengths of 2.2280(15) Å are typical and compare well with $[Cu(PCy_3)_2][PF_6]$, which was prepared by Che *et al.*[18] In that complex the crystal structure reveals a two-coordinate linear copper(I) structure, with Cu–P bond lengths of 2.213(1) and 2.313(1) Å, and a much larger P–Cu–P angle of 179.47(3)°, consistent with a linear geometry and ionic PF_6^-.[18] However, when the counter-ions tetrafluoroborate and perchlorate were employed, three-coordinate structures were obtained (similar to **5a**, structure **B**) with copper–fluorine and copper–oxygen distances of 2.420(6) and 2.220(7) Å and P–Cu–P angles of 159.98(8)° and 144.46(6)° respectively.[23,24] Willet *et al.* showed

that dicyclohexylphenylphosphine (which is the closest analogue to **3a** and **3b**) produced $[Cu(PCy_2Ph)_2][ClO_4]$ with the perchlorate anion, but with tetrafluoroborate a different copper(I) complex formed, $[Cu(PCy_2Ph)_2(F–BF_3)]$. Currently the crystal structures are not known to confirm whether the counter-ions have any significant coordinating interaction.[25]

Silver. Treatment of a dichloromethane solution of (1,5-cyclooctadiene)hexafluoroacetylacetonatosilver(I) ($[Ag(\eta^2{:}\eta^2\text{-cod})(hfa)]$) with two equivalents of **2a**/**2b** or **3a**/**3b** led to the formation of the neutral silver(I) complexes $[Ag(\mathbf{2a}/\mathbf{2b})_2(hfa)]$ (**6a** and **6b**) and $[Ag(\mathbf{3a}/\mathbf{3b})_2(hfa)]$ (**7a** and **7b**), as depicted in Scheme 3. Two phosphines coordinate to the silver, displacing the labile 1,5-cyclooctadiene, to give the products in nearly quantitative yields. Silver has two NMR-active isotopes, ^{107}Ag (I = 1/2, natural abundance 52%) and ^{109}Ag (I = 1/2, natural abundance 48%), therefore the expected $^{31}P\{^1H\}$ NMR spectra for **6a**/**6b** and **7a**/**7b** would consist of two doublets arising from $^{107}Ag–P$ and $^{109}Ag–P$ spin–spin coupling.[26]

Phosphine coordination resulted in a downfield shift of the $^{31}P\{^1H\}$ NMR signal at room temperature from δ −5.5 ppm for the free phosphines **2a**/**2b** to broad peaks at δ 10.2 and 6.6 ppm for the complexes **6a** and **6b** respectively (Fig. 5 and ESI†); the signal was a broad singlet at elevated temperatures in both cases, which likely results from rapid phosphine exchange.[26] This lability is reduced at low temperatures and the Ag–P coupling can be observed.[26]

At low temperature (−40 °C) two doublets appeared; $^1J_{107AgP}$ = 444 Hz and $^1J_{109AgP}$ = 511 Hz, and $^1J_{107AgP}$ = 446 Hz and $^1J_{109AgP}$ = 507 Hz coupling constants were observed for **6a** and **6b** respectively; these values are typical for silver(I) complexes with two phosphines bound[26,27] and compare well to $[Ag(PEt_3)_2(hfa)]$ ($^1J_{107AgP}$ = 468 Hz).[28] For both **6a** and **6b** a second set of two low-intensity doublets was observed at −40 °C and indicates that a second silver species was present in solution. For these signals the following Ag–P couplings were measured: $^1J_{107AgP}$ = 696 Hz and $^1J_{109AgP}$ = 803 Hz, and $^1J_{107AgP}$ = 590 Hz and $^1J_{109AgP}$ = 677 Hz for **6a** and **6b** respectively. The increase in Ag–P coupling constants indicates a change in the hybridisation state of the silver(I) complex[26,27] and is attributed to $[Ag(\mathbf{2a}/\mathbf{2b})(hfa)]$ with only one phosphine ligand bound. The coupling constants are similar to the reported values for $[Ag(PR_3)(hfa)]$ (R = Ph, Me, Et): $^1J_{107AgP}$ = 700–760 Hz.[28,29]

Puddephatt *et al.* reported that an equilibrium is established on the addition of excess phosphine to $[Ag(PR_3)(hfa)]$ complexes and showed that the Ag–hfa bonding is more ionic when extra phosphines are present.[28,30] Mass spectrometry confirmed the $[Ag(\mathbf{2a}/\mathbf{2b})_2]^+$ product, giving peaks at m/z of 1469.6056 (**6a**) and 1217.5443 (**6b**), with loss of the hfa ligand. Low-intensity peaks at 786.2561 and 663.2251 were also observed, which correspond to $[Ag(\mathbf{2a}/\mathbf{2b})]^+$, in addition to peaks at 2148.9477 and 1777.8560 for the tris-cations $[Ag(\mathbf{113a}/\mathbf{113b})_3]^+$, but these latter species were not detected by NMR spectroscopy.

On coordination of the dicyclohexyl phosphines **3a** and **3b** the $^{31}P\{^1H\}$ NMR signals at room temperature were also shifted downfield for the complexes **7a** and **7b**; however, instead of a broad singlet, two broadened doublets were observed at δ 23.7 ppm and δ 23.9 ppm for **7a** and **7b** respectively (Fig. 6 and ESI†). The following Ag–P coupling constants were observed for **7a** and **7b** respectively: $^1J_{107AgP}$ = 453 Hz and $^1J_{109AgP}$ = 517 Hz, and $^1J_{107AgP}$ = 453 Hz and $^1J_{109AgP}$ = 519 Hz. At higher temperatures (120 °C) **7a** and **7b** gave a broad singlet.

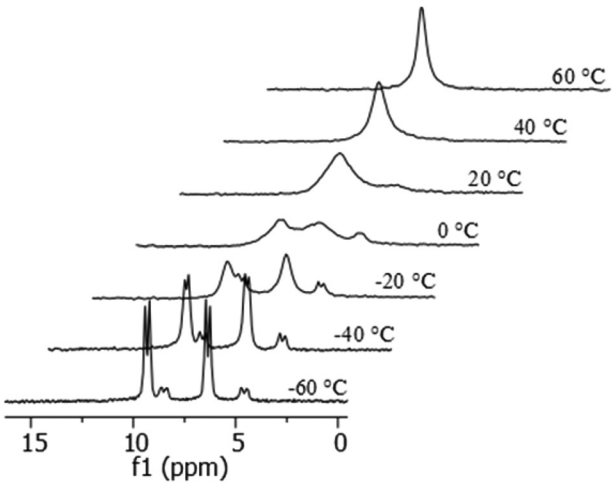

Fig. 5 $^{31}P\{^1H\}$ VT NMR of $[Ag(\mathbf{2b})_2(hfa)]$ **6b**, in d_8-toluene.

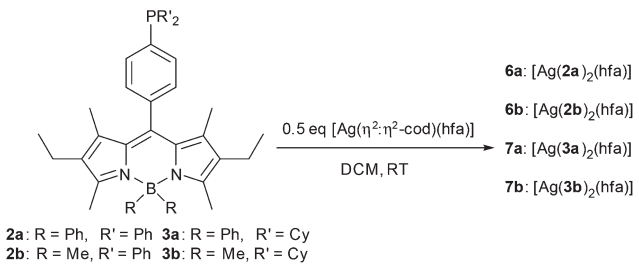

Scheme 3 Synthesis of the silver(I) complexes **6a**/**6b** and **7a**/**7b**.

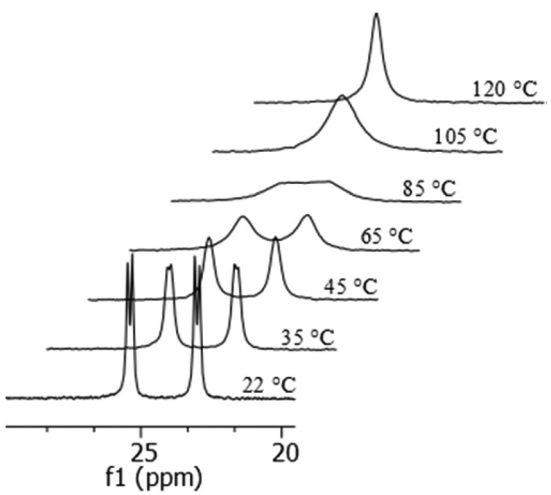

Fig. 6 $^{31}P\{^1H\}$ VT NMR of $[Ag(\mathbf{3b})_2(hfa)]$ **7b**, in d_{10}-*o*-xylene.

The observation of Ag–P coupling at room temperature was unusual since the rapid exchange of the phosphine ligands usually causes this coupling to be averaged to zero; this ligand exchange is normally slowed down by cooling the solution to low temperatures (as is the case for **6a** and **6b**).[27] However, the observation of Ag–P coupling at room temperature has been reported previously, where the phosphine is sterically hindered or chelating.[27,31] Phosphines **3a** and **3b** are also bulky which may explain the lower rate of phosphine exchange and the observation of Ag–P coupling. The electrospray mass spectra gave peaks for $[M - (hfa)]^+$ at *m*/*z* of 1489.7998 for **7a**, and 1242.7354 for **7b**. Complexes **6a** and **7b** were also characterised by X-ray crystallography (Fig. 7). The complexes have neutral silver(I) tetrahedral four-coordinate geometries with two phosphines and one hfa ligand bound to the metal. The Ag–P bond lengths of 2.4255(10) Å and 2.4028(13) Å are typical for silver(I) phosphine complexes.[25,30,32] The complexes are somewhat distorted, shown by the P–Ag–P, P–Ag–O and O–Ag–O bond angles (Fig. 7 caption). The synthesis of a related four-coordinate silver(I) complex $[Ag(PPh_3)_2(hfa)]$ has been reported in a similar fashion, but currently no crystal structure is known.[33]

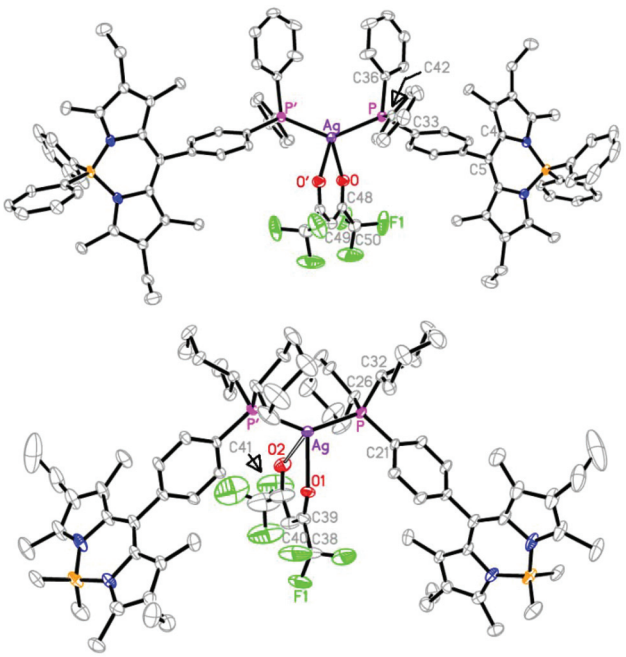

Fig. 7 Molecular structures of **6a** (top) and **7b** (bottom). Hydrogen atoms omitted for clarity. Selected bond distances [Å] and angles [°]: **6a** – Ag–P 2.4255(10), Ag–O 2.407(3), P–C33 1.833(4), P–C36 1.824(4), P–C42 1.825(4), O–C48 1.230(5), C48–C49 1.394(6), C48–C50 1.528(7), F1–C50 1.281(6), C4–C5 1.394(5); P–Ag–P′ 135.24(5), P–Ag–O 102.34(8), O–Ag–O′ 76.40(15), Ag–P–C33 119.40(13), Ag–P–C36 114.02(13), Ag–P–C42 110.39(13), C33–P–C36 101.79(17), C36–P–C42 103.39(19), Ag–O–C48 129.9(3), O–C48–C49 129.3(5), O–C48–C50 112.9(4), C49–C48–C50 117.8(5). **7b** – Ag–P 2.4028(13), Ag–O1 2.337(6), Ag–O2 2.718(8), P–C21 1.813(5), P–C26 1.826(5), P–C32 1.844(5), O1–C39 1.231(11), O2–C41 1.233(13), C39–C40 1.392(14), C40–C41 1.403(14), F1–C38 1.345(16); P–Ag–P′ 141.99(7), P–Ag–O1 112.2(4), O1–Ag–O2 71.93(3), Ag–P–C21 115.98(17), Ag–P–C26 111.93(18), Ag–P–C32 110.70(17), C21–P–C32 103.8(2), C26–P–C32 108.0(3), Ag–O1–C39 135.9(7), O1–C39–C40 132.0(11), O1–C39–C38 111.9(10), C38–C39–C40 115.7(10). Primes denote symmetry-generated atoms.

Gold. Treatment of chloro(tetrahydrothiophene)gold(I) [AuCl(tht)] with one equivalent of **2a**/**2b** or **3a**/**3b** in dichloromethane led to the formation of the neutral gold(I) complexes [AuCl(**2a**/**2b**)] (**8a** and **8b**) and [AuCl(**3a**/**3b**)] (**9a** and **9b**), as depicted in Scheme 4. In each case one phosphine coordinates to the gold, replacing the labile tht ligand; purification was achieved by column chromatography, resulting in high yields of 75–91%.

Coordination of the phosphines resulted in a downfield shift of the $^{31}P\{^1H\}$ NMR signal of the free phosphines **2a**/**2b** and **3a**/**3b** to δ 33.2/33.3 and 51.4/51.6 ppm for the complexes **8a**/**8b** and **9a**/**9b** respectively. Complexes **8a**, **9a** and **9b** were also characterised by X-ray crystallography (Fig. 8 and ESI†). The solid-state structures show them to be gold(I) two-coordinate linear complexes, as expected.

The Au–P and Au–Cl bond lengths are typical for gold(I) compounds (Fig. 8 caption).[34] The P–Au–Cl bond angles of 177.24(14)°, 178.27(5)° and 177.55(3)° for **8a**, **9a** and **9b** respectively are close to the ideal 180° for a linear complex. The analogous complex to **8a**/**8b**, $[AuCl(PPh_3)]$, prepared from triphenylphosphine and chloroauric acid, has a slightly longer P–Au bond length (2.235(3) Å), and a slightly larger Au–P–Cl bond angle than **8a** (179.68(8)°).[34a] The analogous dicyclohexylphenylphosphine complex, $[AuCl(PCy_2Ph)]$, made from the ligand and a reaction mixture of tetrachloroauric acid and 2,2′-thiodiethanol, has P–Au and P–Cl bond lengths of 2.234(2)

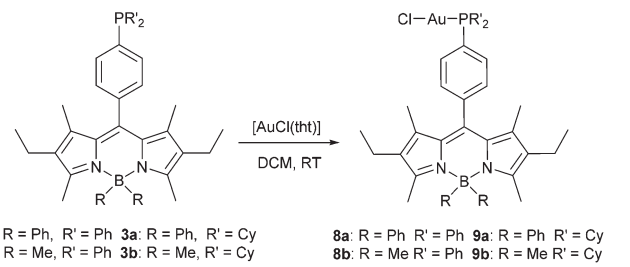

Scheme 4 Synthesis of the gold(I) complexes **8a**/**8b** and **9a**/**9b**.

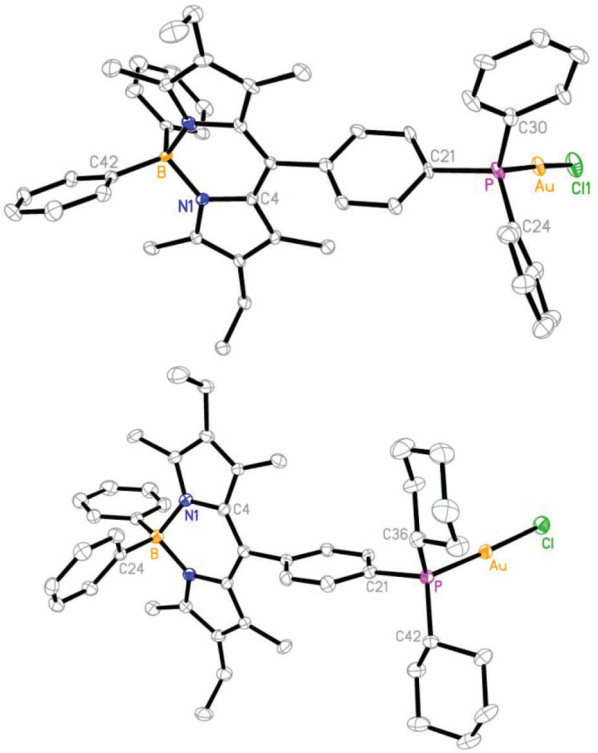

Fig. 8 View of the molecular structure of **8a** (top) and **9a** (bottom). Hydrogen atoms have been omitted for clarity. Selected bond distances [Å] and angles [°]: **8a** – Au–P 2.223(3), Au–Cl1 2.281(3), P–C21 1.816(12), P–C24 1.817(14), P–C30 1.810(13), C4–N1 1.400(16), N1–B 1.566(17), B–C42 1.65(2); P–Au–Cl1 177.24(14), C21–P–C24 108.1(6), C21–P–C30 104.7(6), C24–P–C30 103.1(6), Au–P–C21 110.7(4), Au–P–C24 113.5(5), Au–P–C30 116.0(4). **9a** – Au–P 2.2351(13), Au–Cl 2.2875(13), P–C21 1.817(4), P–C36 1.838(5), P–C42 1.845(4), C4–N1 1.390(5), N1–B 1.574(6), B–C24 1.646(7); P–Au–Cl 178.27(5), C21–P–C36 102.2(2), C21–P–C42 104.0(2), C36–P–C42 109.8(2), Au–P–C21 112.53(15), Au–P–C36 113.34(16), Au–P–C42 113.90(17).

and 2.281(3) Å respectively and an Au–P–Cl bond angle of 178.3(1)°, very similar to **9a**/**9b**.[34b]

Optical properties

After the synthesis of several group 11 metal complexes of **2a**/**2b** and **3a**/**3b**, it was important to determine and understand their photophysical properties. Our initial concern was whether the phosphorus donor[4] or the heavy metals[35] themselves would quench the fluorescence of the Bodipy fluorophore, which has been shown to occur for other fluorophores in phosphorus systems. Photophysical data were collected for all ligands and complexes in dry degassed tetrahydrofuran to minimise photobleaching and phosphine oxidation in solution (Table 1).

The four phosphine ligands **2a**/**2b** and **3a**/**3b** all show a typical Bodipy profile[6] with absorption maxima at either 517/513 nm or 518/512 nm depending on the groups at the boron centre; changing from diphenyl to dimethyl causes a hypsochromic shift of the absorption maxima (4–6 nm). The lowest energy maximum is assigned to the S_0–S_1 (π–π*) tran-

Table 1 Photophysical data for phosphines **2a**/**2b**, **3a**/**3b** and the group 11 complexes **4a**/**4b**–**9a**/**9b**[a]

Compound	λ_{abs} (nm)	λ_{em} (nm)	ε (M^{-1} cm^{-1})	Φ_F
2a	517	534	77 000	0.042
4a (Cu)	518	535	133 000	0.038
6a (Ag)	518	535	151 000	0.036
8a (Au)	519	538	76 000	0.034
2b	513	527	92 000	0.29
4b (Cu)	513	528	167 000	0.29
6b (Ag)	513	528	155 000	0.26
8b (Au)	514	529	74 000	0.20
3a	518	533	77 000	0.073
5a (Cu)	518	534	143 000	0.069
7a (Ag)	518	534	141 000	0.070
9a (Au)	519	536	78 000	0.058
3b	512	526	82 000	0.44
5b (Cu)	512	527	171 000	0.42
7b (Ag)	513	527	157 000	0.43
9b (Au)	514	529	85 000	0.39

[a] Measured in dry degassed tetrahydrofuran at room temperature. Fluorescence quantum yields were measured with respect to 4,4-difluoro-8-phenyl-1,3,5,7-tetramethyl-2,6-diethyl-4-bora-3a,4a-diaza-*s*-indacene.[36]

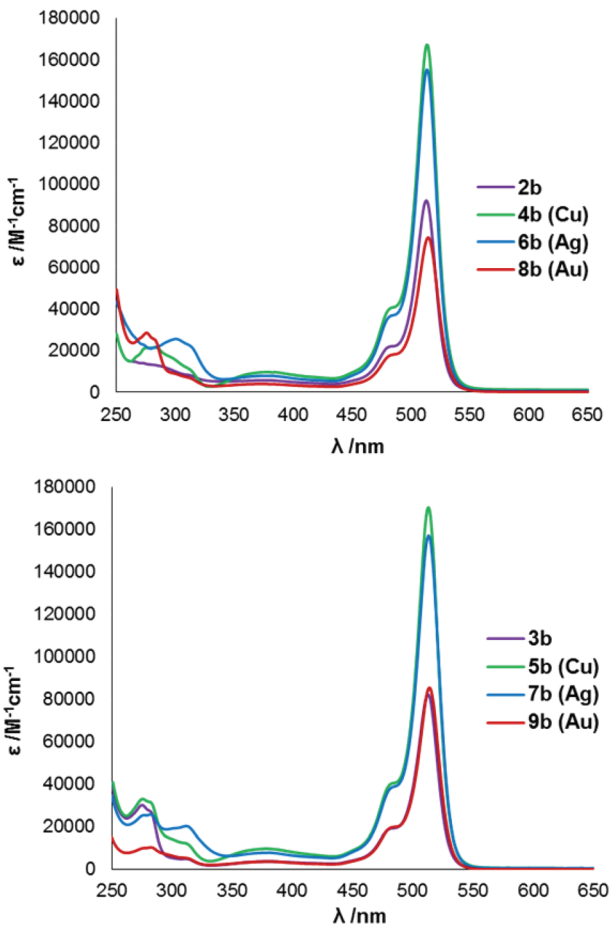

Fig. 9 Top: absorption spectra of triarylphosphine **2b** and its complexes [Cu(**2b**)$_2$(CH$_3$CN)][PF$_6$] **4b**, [Ag(**2b**)$_2$(hfa)] **6b** and [AuCl(**2b**)] **8b**. Bottom: absorption spectra of aryldialkylphosphine **3b** and its complexes [Cu(**3b**)$_2$(CH$_3$CN)][PF$_6$] **5b**, [Ag(**3b**)$_2$(hfa)] **7b** and [AuCl(**3b**)] **9b**. All measured in dry degassed tetrahydrofuran at room temperature (concentrations range from 3.0 × 10^{-6} to 1.1 × 10^{-5} M, see ESI†).

sition for the Bodipy core. All the ligands have typically high molar absorption coefficients, ranging from 77 000 to 92 000 M^{-1} cm^{-1}.[6] Secondly, a lower intensity, broader absorption band can be seen between 370 and 385 nm (ε = 3000–10 000 M^{-1} cm^{-1}), which is attributed to the S_0–S_2 (π–π^*) transition of the Bodipy core. There are also low-intensity, high-energy peaks centred between 250–300 nm for the dicyclohexyl derivatives **3a**/**3b**. The absorption spectra for phosphines **2b**/**3b** and their complexes are given in Fig. 9; the corresponding spectra for **2a**/**3a** and their complexes is given in the ESI.†

Room-temperature fluorescence of the phosphine ligands was readily detected, with maxima of 534/527 nm or 533/526 nm, again depending on the boron substituents (Fig. 10). The Stokes shifts of 14–17 nm are small, which is common for the Bodipy fluorophore, and suggests that only small structural changes occur on excitation.[6] The fluorescence quantum yields of **2b** (0.29) and **3b** (0.44) are typically high for Bodipy molecules and compare well to the parent Bodipy **10b** (0.35, ESI†), which shows the phosphorus donor does not quench the fluorescence.

This is unusual and, as with our previously reported Bodipy primary phosphines,[15] contradicts several phosphine examples.[4] However, it is perhaps to be expected, given that the DFT calculations (see Fig. 11 and ESI†) show there is no phosphorus character in the HOMO, HOMO−1 or HOMO−2 for **2a** and **3a**, nor in the HOMO or HOMO−1 for **2b** and **3b**, and that the energy difference between the HOMO and the first phosphorus-containing orbital is 0.9 eV for all the phosphine ligands (Fig. 11 and ESI†). The quantum yield for **3b** is, perhaps surprisingly, also higher than that of the parent Bodipy which has no substituents on the *meso* phenyl ring (**3b** = 0.44 and **10b** = 0.35). More detailed investigations into a Bodipy phosphine series could reveal how the quantum yield is affected by both the electronic and steric nature of the substituents on the phosphorus. Changing the methyl groups at the boron atom for phenyl groups severely quenches the fluorescence (compare **2b**: Φ_F = 0.29 to **2a**: Φ_F = 0.042), which is consistent with our previous findings.[15] The absorption spectra of the complexes are very similar to those of the un-

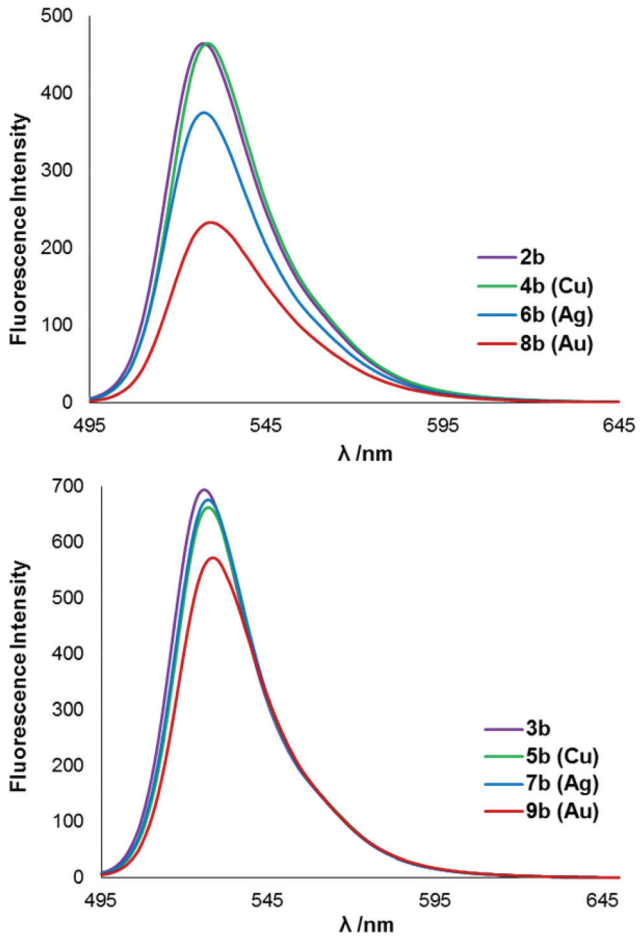

Fig. 10 Top: emission spectra of triarylphosphine **2b** and its complexes [Cu(**2b**)$_2$(CH$_3$CN)][PF$_6$] **4b**, [Ag(**2b**)$_2$(hfa)] **6b** and [AuCl(**2b**)] **8b**. Bottom: emission spectra of aryldialkylphosphine **3b** and its complexes [Cu(**3b**)$_2$(CH$_3$CN)][PF$_6$] **5b**, [Ag(**3b**)$_2$(hfa)] **7b** and [AuCl(**3b**)] **9b**. All measured in dry degassed tetrahydrofuran at room temperature, excitation wavelength = 485 nm, concentrations range from 1.9 × 10^{-6} to 4.0 × 10^{-6} M, see ESI†).

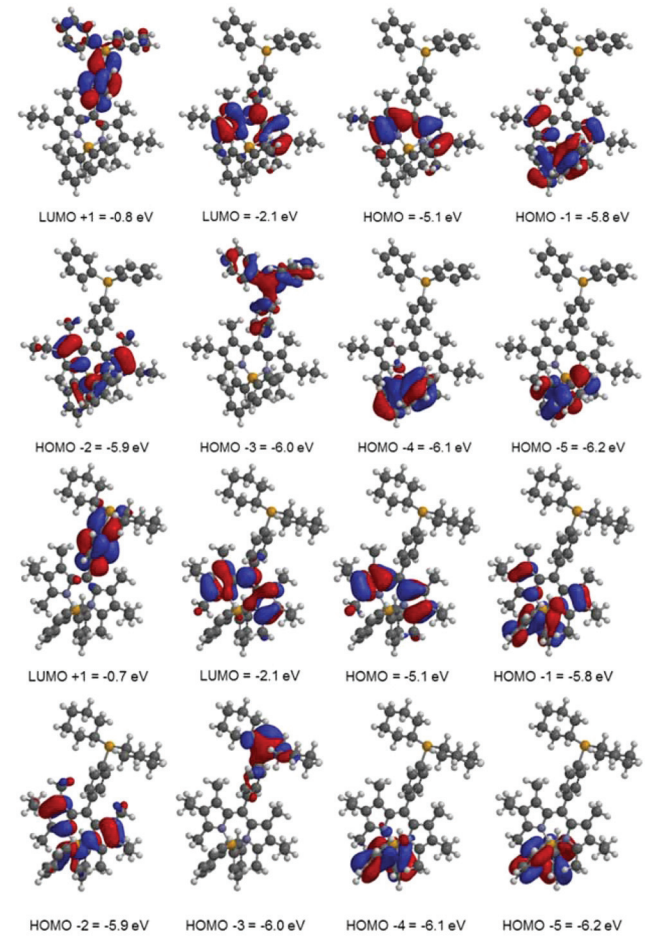

Fig. 11 Calculated molecular orbital surfaces of the triarylphosphine **2a** (top two rows) and the aryldialkylphosphine **3a** (bottom two rows) from LUMO+1 to HOMO−5.

coordinated ligands (Fig. 9); wavelengths of the low energy transition fall in the range 519–512 nm. The corresponding molar extinction coefficients are large for the copper (**4–5**) and silver (**6–7**) complexes (ε = 133 000–171 000 M^{-1} cm^{-1}), due to the presence of two Bodipy ligands; the monodentate gold complexes (**8–9**) retain similar values to the free ligands (ε = 74 000–85 000 M^{-1} cm^{-1}).

The fluorescence spectra of the complexes **4b–9b** are displayed in Fig. 10. On complexation, the fluorescence quantum yields are generally retained, with only a slight decrease observed on descending the group (for instance **2b**: Φ_F = 0.29, **8b**: Φ_F = 0.20). The gold species (**8–9**) have the lowest relative quantum yields, likely due to the heavy atom effect. Quenching is less pronounced for the aryldialkylphosphine complexes of **3b** compared to those of the triarylphosphine **2b** (Table 1, Fig. 10) and all three metal complexes of **3b** have higher quantum yields than the parent Bodipy **10b** (Φ_F = 0.35). It is noteworthy that Gray *et al.* reported group 11 complexes which contained separated azadipyrromethene and triphenylphosphine ligands; however, the molar extinction coefficient and fluorescence quantum yields are significantly lower in those cases, 30 000–65 000 M^{-1} cm^{-1} and 0.0024–0.0039 respectively.[37]

Conclusions

The synthesis of fluorescent monodentate triaryl and aryldialkyl tertiary phosphines has been achieved in excellent yields *via* the lithiation of the Bodipy aryl bromides **1a**/**1b**, and subsequent addition of the relevant chlorophosphine. This route may be transferable to a range of aryl and alkyl chlorophosphines and thus could be an excellent route to a library of new Bodipy tertiary phosphines. The photophysical properties of the phosphines are intriguing; the fluorescence is not quenched significantly compared to their precursor and, in fact, in the case of aryldialkylphosphines **3a** and **3b**, the emission is enhanced in comparison to their parent Bodipys **10a** and **10b** (see ESI†). The novel phosphines **2a**/**2b** and **3a**/**3b** readily coordinate to low-oxidation-state coinage metals at room temperature in nearly quantitative yield; upon coordination, the fluorescence of the phosphines is not significantly quenched. These novel ligands and their complexes have potential applications in medicinal imaging, as the fluorescent Bodipy functionality will facilitate cell imaging. Several group 11 metal phosphine complexes have shown cytotoxic properties against several cancer cell lines,[8–10] and our novel derivatives may well display similar attributes. Future work will focus on their use in diagnostic imaging and therapy.

Experimental

All air- and/or water-sensitive reactions were performed under a nitrogen atmosphere using standard Schlenk line techniques. Tetrahydrofuran and diethyl ether were dried over sodium/benzophenone. Dichloromethane and chloroform were dried over calcium hydride; all solvents were distilled prior to use. Hexane and pentane were purchased in an anhydrous state. Most starting materials were purchased from Aldrich, Acros Organics, Alfa Aesar or Strem and used as received. 4,4-Difluoro-8-phenyl-1,3,5,7-tetramethyl-2,6-diethyl-4-bora-3a,4a-diaza-*s*-indacene,[36] the arylbromides **1a**/**1b**[15] and [AuCl(tht)][38] were prepared according to literature procedures.

Flash chromatography was performed on silica gel from Fluorochem (silica gel, 40–63 μ, 60 Å, LC301). Thin-layer chromatography was performed on Fisher aluminium-based plates with silica gel and fluorescent indicator (254 nm). Infrared spectra were recorded on a Varian 800 FT-IR spectrometer and mass spectrometry was carried out by the EPSRC National Mass Spectrometry Service Centre, Swansea. ^1H, $^{13}C\{^1H\}$, $^{31}P\{^1H\}$, $^{19}F\{^1H\}$ and $^{11}B\{^1H\}$ NMR spectra were recorded on a JEOL Lambda 500 (^1H 500.16 MHz) or JEOL ECS-400 (^1H 399.78 MHz) spectrometer at room temperature (21 °C) using the indicated solvent as internal reference, unless specified otherwise; ^1H and ^{13}C shifts were relative to tetramethylsilane, ^{31}P relative to 80% H_3PO_4, ^{11}B relative to $BF_3{\cdot}Et_2O$ and ^{19}F relative to $CFCl_3$. It is worth noting that, as for dicyclohexylphenylphosphine,[39] six unique cyclohexyl carbon signals are seen in the $^{13}C\{^1H\}$ NMR spectra for phosphines **3a** and **3b** and their respective complexes. The six signals arise as the two cyclohexyl rings are equivalent but the carbon atoms that are symmetrically equivalent are diastereotopic; these diastereotopic carbon atoms are also non-equivalent with respect to P–C coupling constants.

All calculations were carried out using Spartan 10 software.[40] Full geometry optimizations of the studied compounds were performed using density functional theory with a B3LYP/6-31G* basis set. A vibrational analysis was performed at the same level to characterize calculated structures as minima.

Absorption spectra were recorded with a Hitachi Model U-3310 spectrophotometer while fluorescence studies were recorded with a Hitachi F-4500 fluorescence spectrophotometer. Solvents used for spectroscopic experiments were spectrophotometric grade. Absorption and emission spectra were recorded in dry degassed tetrahydrofuran solution at room temperature. Fluorescence quantum yields were measured with respect to 4,4-difluoro-8-phenyl-1,3,5,7-tetramethyl-2,6-diethyl-4-bora-3a,4a-diaza-*s*-indacene (Φ_F = 0.76, λ_{abs} = 524 nm, λ_{em} = 537 nm, ε = 86 000 M^{-1} cm^{-1}, tetrahydrofuran).[36] Dyes were excited at 485 nm and excitation slits set to 5 nm.

8-((4-Diphenylphosphino)phenyl)-4,4-diphenyl-1,3,5,7-tetramethyl-2,6-diethyl-4-bora-3a,4a-diaza-*s*-indacene (2a)

8-(4-Bromophenyl)-4,4-diphenyl-1,3,5,7-tetramethyl-2,6-diethyl-4-bora-3a,4a-diaza-*s*-indacene (0.50 g, 0.87 mmol) was dissolved in anhydrous diethyl ether (40 mL) and cooled to −78 °C. *n*-BuLi (0.38 mL, 0.96 mmol, 2.5 M in hexane) was added dropwise over five minutes and the reaction was warmed to room temperature over 45 min. The solution was cooled back to −78 °C and chlorodiphenylphosphine (0.17 mL, 0.96 mmol) was added dropwise. The reaction

mixture was allowed to warm up to room temperature and was stirred for a further two hours. It was washed with water and extracted with diethyl ether (3 × 30 mL). The combined organic fractions were washed with brine (30 mL) and dried over magnesium sulfate. The solvent was removed *in vacuo* to yield a red/orange solid. The compound was purified using column chromatography on silica gel (toluene–hexane 2 : 3, R_f = 0.4) and gave an orange solid (0.50 g, 84%). A sample suitable for X-ray crystallographic analysis was obtained from chloroform–pentane. **^{1}H NMR** (400 MHz, $CDCl_3$) δ 7.45–7.41 (m, 7H), 7.40–7.35 (m, 11H), 7.29–7.24 (m, 4H), 7.22–7.19 (m, 2H), 2.26 (q, $^3J_{HH}$ = 7.3 Hz, 4H), 1.82 (s, 6H), 1.44 (s, 6H), 0.94 (t, $^3J_{HH}$ = 7.3 Hz, 6H) ppm; **^{13}C{^{1}H} NMR** (100 MHz, $CDCl_3$) δ 153.0, 150.8 (br), 140.0, 137.9 (d, J_{CP} = 11.5 Hz), 137.3, 136.7 (d, J_{CP} = 10.5 Hz), 135.0, 133.8, 133.6, 133.4, 132.8, 130.6, 129.0, 128.9, 128.6 (d, J_{CP} = 6.7 Hz), 127.1, 125.4, 17.3, 14.7, 14.5, 12.1 ppm; **^{31}P{^{1}H} NMR** (162 MHz, $CDCl_3$) δ −5.5 ppm; **^{11}B{^{1}H} NMR** (128 MHz, $CDCl_3$) δ −1.0 ppm; **IR** (neat): $\tilde{\nu}$ = 2958 (w), 1542 (s), 1472 (s), 1396 (s), 1308 (m), 1170 (m), 1143 (m), 1061 (m), 971 (s), 775 (s) cm^{-1}; **HRMS** (ESI$^+$) exact mass calcd for $C_{47}H_{47}N_2B_1P_1$ [M + H]$^+$ requires *m*/*z* 681.3544, found *m*/*z* 681.3570 (2.6 ppm).

8-((4-Diphenylphosphino)phenyl)-4,4-dimethyl-1,3,5,7-tetramethyl-2,6-diethyl-4-bora-3a,4a-diaza-*s*-indacene (2b)

Prepared in the same manner as for **2a** using 0.50 g (1.11 mmol) of 8-(4-bromophenyl)-4,4-dimethyl-1,3,5,7-tetramethyl-2,6-diethyl-4-bora-3a,4a-diaza-*s*-indacene, 0.49 mL (1.22 mmol) of *n*-BuLi (2.5 M in hexane) and 0.22 mL (1.22 mmol) of chlorodicyclohexylphosphine. The compound was purified using column chromatography on silica gel (chloroform–hexane 1 : 5, R_f = 0.3) to yield an orange solid (0.37 g, 60%). **^{1}H NMR** (400 MHz, $CDCl_3$) δ 7.45–7.42 (m, 2H), 7.41–7.35 (m, 10H), 7.34–7.30 (m, 2H), 2.47 (s, 6H), 2.35 (q, $^3J_{HH}$ = 7.3 Hz, 4H), 1.36 (s, 6H), 1.01 (t, $^3J_{HH}$ = 7.3 Hz, 6H), 0.30 (s, 6H) ppm; **^{13}C{^{1}H} NMR** (100 MHz, $CDCl_3$) δ 150.6, 139.8, 137.9, 137.8, 136.7 (d, J_{CP} = 11.5 Hz), 133.8, 133.6, 133.5, 132.4, 132.1, 132.0, 128.8, 128.5 (d, J_{CP} = 6.7 Hz), 17.4, 14.7, 14.5, 11.9, 10.4 (br) ppm; **^{31}P{^{1}H} NMR** (162 MHz, $CDCl_3$) δ −5.5 ppm; **^{11}B{^{1}H} NMR** (128 MHz, $CDCl_3$) δ −1.9 ppm; **IR** (neat): $\tilde{\nu}$ = 2924 (w), 2863 (w), 1552 (s), 1455 (m), 1372 (w), 1314 (s), 1170 (s), 1144 (s), 1064 (m), 977 (s) cm^{-1}; **HRMS** (EI$^+$) exact mass calcd for $C_{37}H_{43}N_2B_1P_1$ [M + H]$^+$ requires *m*/*z* 556.3288, found *m*/*z* 556.3294 (1.1 ppm).

8-((4-Dicyclohexylphosphino)phenyl)-4,4-diphenyl-1,3,5,7-tetramethyl-2,6-diethyl-4-bora-3a,4a-diaza-*s*-indacene (3a)

Prepared in the same manner as for **2a** using 0.50 g (0.87 mmol) of 8-(4-bromophenyl)-4,4-diphenyl-1,3,5,7-tetramethyl-2,6-diethyl-4-bora-3a,4a-diaza-*s*-indacene, 0.38 mL (0.96 mmol) of *n*-BuLi (2.5 M in hexane) and 0.21 mL (0.96 mmol) of chlorodicyclohexylphosphine. The compound was purified using column chromatography on silica gel (dichloromethane–hexane 1 : 4, R_f = 0.3) to yield an orange solid (0.42 g, 69%). **^{1}H NMR** (500 MHz, $CDCl_3$) δ 7.59–7.56 (m, 2H), 7.41–7.33 (m, 6H), 7.23–7.17 (m, 6H), 2.22 (q, $^3J_{HH}$ = 7.8 Hz, 4H), 1.99–1.66 (m, 12H), 1.77 (s, 6H), 1.36–1.02 (m, 10H), 1.33 (s, 6H), 0.90 (t, $^3J_{HH}$ = 7.8 Hz, 6H) ppm, **^{13}C{^{1}H} NMR** (126 MHz, $CDCl_3$) δ 153.1, 150.8 (br), 140.5, 137.6, 135.2, 135.1, 135.0, 134.0, 133.0, 130.8, 128.4 (d, J_{CP} = 7.6 Hz), 127.2, 125.6, 32.2 (d, $^1J_{CP}$ = 11.5 Hz), 30.1 (d, $^2J_{CP}$ = 16.3 Hz), 28.7 (d, $^2J_{CP}$ = 6.7 Hz), 27.3 (d, $^3J_{CP}$ = 12.5 Hz), 27.1 (d, $^3J_{CP}$ = 7.7 Hz), 26.7, 17.5, 14.8, 14.7, 12.1 ppm; **^{31}P{^{1}H} NMR** (202 MHz, $CDCl_3$) δ 2.7 ppm; **^{11}B{^{1}H} NMR** (128 MHz, $CDCl_3$) δ −0.7 ppm; **IR** (neat): $\tilde{\nu}$ = 2925 (m), 2850 (m), 1548 (s), 1474 (m), 1384 (m), 1307 (s), 1168 (s), 1110 (m), 973 (s) cm^{-1}; **HRMS** (AP$^+$) calcd for $C_{47}H_{59}B_1N_2P_1$ [M + H]$^+$ requires *m*/*z* 692.4540, found *m*/*z* 692.4560 (2.9 ppm).

8-((4-Dicyclohexylphosphino)phenyl)-4,4-dimethyl-1,3,5,7-tetramethyl-2,6-diethyl-4-bora-3a,4a-diaza-*s*-indacene (3b)

Prepared in the same manner as for **2a** using 0.50 g (1.11 mmol) of 8-(4-bromophenyl)-4,4-dimethyl-1,3,5,7-tetramethyl-2,6-diethyl-4-bora-3a,4a-diaza-*s*-indacene, 0.49 mL (1.22 mmol) of *n*-BuLi (2.5 M in hexane) and 0.27 mL (1.22 mmol) of chlorodicyclohexylphosphine. The compound was purified using column chromatography on silica gel (chloroform–hexane 1 : 4, R_f = 0.4) to yield an orange solid (0.39 g, 62%). **^{1}H NMR** (400 MHz, $CDCl_3$) δ 7.47 (m, 2H), 7.21 (d, $^3J_{HH}$ = 8.2 Hz, 2H), 2.37 (s, 6H), 2.23 (q, $^3J_{HH}$ = 7.3 Hz, 4H), 1.90–1.56 (m, 12H), 1.90 (s, 6H), 1.30–0.78 (m, 10H), 0.90 (t, $^3J_{HH}$ = 7.3 Hz, 6H), 0.21 (s, 6H) ppm; **^{13}C{^{1}H} NMR** (100 MHz, $CDCl_3$) δ 150.6, 140.2, 137.9, 135.0 (d, J_{CP} = 19.2 Hz), 134.7 (d, J_{CP} = 19.2 Hz), 133.8, 132.5, 129.1, 128.3 (d, J_{CP} = 7.7 Hz), 32.1 (d, $^1J_{CP}$ = 12.5 Hz), 29.9 (d, $^2J_{CP}$ = 16.3 Hz), 28.7 (d, $^2J_{CP}$ = 6.7 Hz), 27.4 (d, $^3J_{CP}$ = 12.5 Hz), 27.1 (d, $^3J_{CP}$ = 6.7 Hz), 26.7, 17.6, 14.8, 14.4, 11.9, 10.5 (br) ppm; **^{31}P{^{1}H} NMR** (162 MHz, $CDCl_3$) δ 2.8 ppm; **^{11}B{^{1}H} NMR** (128 MHz, $CDCl_3$) δ −2.1 ppm; **IR** (neat): $\tilde{\nu}$ = 2927 (w), 2856 (w), 1551 (s), 1448 (m), 1321 (m), 1171 (s), 1145 (s), 946 (s) cm^{-1}; **HRMS** (AP$^+$) calcd for $C_{37}H_{55}B_1N_2P_1$ [M + H]$^+$ requires *m*/*z* 568.4227, found *m*/*z* 568.4226 (0.1 ppm).

[Cu(2a)$_2$(CH$_3$CN)][PF$_6$] (4a)

Tetrakis(acetonitrile)copper(I)hexafluorophosphate (0.027 g, 0.073 mmol) and 8-(4-diphenylphosphine)phenyl-4,4-diphenyl-1,3,5,7-tetramethyl-2,6-diethyl-4-bora-3a,4a-diaza-*s*-indacene (0.100 g, 0.147 mmol) were added together to anhydrous dichloromethane (3 mL) and stirred under nitrogen for two hours. After removal of solvent an orange solid was produced (0.107 g, 93%). A sample suitable for X-ray crystallographic analysis was obtained from ethanol–pentane. **^{1}H NMR** (500 MHz, $CDCl_3$) δ 7.51–7.47 (m, 4H), 7.46–7.40 (m, 12H), 7.39–7.32 (m, 20H), 7.28–7.22 (*pseudo* t, 8H), 7.21–7.16 (m, 4H), 2.20 (q, $^3J_{HH}$ = 7.3 Hz, 8H), 2.19 (s, 3H), 1.77 (s, 12H), 1.34 (s, 12H), 0.88 (t, $^3J_{HH}$ = 7.3 Hz, 12H) ppm; **^{13}C{^{1}H} NMR** (126 MHz, $CDCl_3$) δ 153.7, 150.3 (br), 139.3, 138.9, 134.6, 134.0, 133.9, 133.5, 133.4, 131.8, 131.0, 130.8, 130.5, 130.0, 129.4, 127.3, 125.7, 120.3, 17.7, 14.8, 14.7, 12.3, 2.31 ppm; **^{31}P{^{1}H} NMR** (202 MHz, $CDCl_3$) δ 0.0 (br), −143.6 (septet, $^1J_{PF}$ = 712.6 Hz) ppm; **^{11}B{^{1}H} NMR** (162 MHz, $CDCl_3$) δ −1.0 ppm; **IR** (neat): $\tilde{\nu}$ = 2960 (w), 2925 (w), 2869 (w), 1548 (s), 1473 (m),

1435 (m), 1397 (m), 1362 (m), 1305 (m), 1263 (w), 1173 (s), 1144 (m), 974 (s) cm^{-1}; **HRMS** (ESI^+) calcd for $C_{94}H_{92}B_2N_4P_2Cu_1$ $[M - C_2H_3N_1]^+$ requires *m*/*z* 1421.6346, found *m*/*z* 1421.6335 (0.8 ppm).

$[Cu(2b)_2(CH_3CN)][PF_6]$ (4b)

Prepared in the same manner as for **4a** using 0.034 g (0.090 mmol) of tetrakis(acetonitrile)copper(I) hexafluorophosphate and 0.100 g (0.180 mmol) of **2b**. Yield 0.115 g (97%). A sample suitable for X-ray crystallographic analysis was obtained from ethanol–pentane. **^{1}H NMR** (500 MHz, $CDCl_3$) δ 7.48 (m, 5H), 7.39 (m, 12H), 7.30 (m, 11H), 2.46 (s, 12H), 2.28 (q, $^3J_{HH}$ = 7.3 Hz, 8H), 2.14 (s, 3H), 1.26 (s, 12H), 0.96 (t, $^3J_{HH}$ = 7.3 Hz, 12H), 0.28 (s, 12H) ppm; **^{13}C{^{1}H} NMR** (126 MHz, $CDCl_3$) δ 151.2, 140.4, 138.6, 134.1, 133.5, 133.1, 133.0, 131.6, 130.9, 130.8, 129.9, 129.4, 128.7, 120.6, 17.5, 14.8, 14.4, 12.1, 10.5 (br), 2.2 ppm; **^{31}P{^{1}H} NMR** (202 MHz, $CDCl_3$) δ 0.1 (br), −143.6 (septet, $^1J_{PF}$ = 712.6 Hz) ppm; **^{11}B{^{1}H} NMR** (128 MHz, $CDCl_3$) δ −1.8 ppm; **IR** (neat): $\tilde{\nu}$ = 2959 (w), 2925 (w), 2869 (w), 1551 (s), 1471 (m), 1435 (m), 1360 (m), 1320 (s), 1264 (w), 1173 (s), 1145 (s), 1112 (m), 1026 (w), 981 (m), 945 (s) cm^{-1}; **HRMS** (ESI^+) calcd for $C_{74}H_{84}B_2N_4P_2Cu_1$ $[M - C_2H_3N_1]^+$ requires *m*/*z* 1173.5720, found *m*/*z* 1173.5927 (0.9 ppm).

$[Cu(3a)_2(CH_3CN)][PF_6]$ (5a)

Prepared in the same manner as for **4a** using 0.027 g (0.072 mmol) of tetrakis(acetonitrile)copper(I) hexafluorophosphate and 0.100 g (0.144 mmol) of **3a**. Yield 0.114 g (97%). A sample suitable for X-ray crystallographic analysis was obtained from chloroform–pentane. **^{1}H NMR** (500 MHz, $CDCl_3$) δ 7.67 (m, 4H), 7.48–7.34 (m, 12H), 7.25–7.18 (m, 12H), 2.42–2.23 (m, 4H), 2.22 (br, 3H), 2.13 (q, $^3J_{HH}$ = 7.3 Hz, 8H), 1.91–1.61 (m, 16H), 1.76 (s, 12H), 1.47–1.06 (m, 24H), 1.36 (s, 12H), 0.83 (t, $^3J_{HH}$ = 7.3 Hz, 12H) ppm; **^{13}C{^{1}H} NMR** (126 MHz, $CDCl_3$) δ 153.8, 150.2 (br), 140.4, 138.7, 134.9 (m), 134.4, 133.9, 133.4, 130.4, 129.7 (m), 127.3, 126.8 (*pseudo* t, J_{CP} = 15.1 Hz), 125.7, 121.9, 31.8 (*pseudo* t, $^1J_{CP}$ = 10.6 Hz), 29.7 (br), 28.6, 26.8 (*pseudo* t, $^3J_{CP}$ = 6.8 Hz), 26.6 (*pseudo* t, $^3J_{CP}$ = 4.8 Hz), 26.2, 17.4, 14.8, 14.7, 12.2, 2.5 ppm; **^{31}P{^{1}H} NMR** (202 MHz, $CDCl_3$) δ 13.4 (br), −143.5 (septet, $^1J_{PF}$ = 712.6 Hz) ppm; **^{11}B{^{1}H} NMR** (128 MHz, $CDCl_3$) δ −0.2 ppm; **IR** (neat): $\tilde{\nu}$ = 2960 (w), 2929 (w), 2854 (w), 1549 (s), 1475 (m), 1449 (w), 1397 (w), 1362 (w), 1304 (m), 1263 (w), 1173 (s), 1145 (m), 1112 (m), 974 (s) cm^{-1}; **HRMS** (ESI^+) calcd for $C_{94}H_{116}B_2N_4P_2Cu_1$ $[M - C_2H_3N_1]^+$ requires *m*/*z* 1445.8224, found *m*/*z* 1445.8197 (1.9 ppm).

$[Cu(3b)_2(CH_3CN)][PF_6]$ (5b)

Prepared in the same manner as for **4a** using 0.033 g (0.088 mmol) of tetrakis(acetonitrile)copper(I) hexafluorophosphate and 0.100 g (0.176 mmol) of **3b**. Yield 0.117 g (96%). A sample suitable for X-ray crystallographic analysis was obtained from chloroform–pentane. **^{1}H NMR** (500 MHz, $CDCl_3$) δ 7.61 (m, 4H), 7.38 (d, $^3J_{HH}$ = 7.3 Hz, 4H), 2.43 (s, 12H), 2.34 (m, 3H), 2.20 (q, $^3J_{HH}$ = 7.3 Hz, 8H), 2.21 (m, 4H), 1.90 (m, 4H), 1.75 (12H), 1.44–1.03 (m, 24H), 1.18 (s, 12H), 0.94 (t, $^3J_{HH}$ = 7.3 Hz, 12H), 0.26 (s, 12H) ppm; **^{13}C{^{1}H} NMR** (126 MHz, $CDCl_3$) δ 151.2, 140.7, 138.4, 134.9, 133.0, 132.9, 129.4, 128.6, 126.6 (*pseudo* t, J_{CP} = 15.2 Hz), 122.5, 31.8 (*pseudo* t, $^1J_{CP}$ = 10.6 Hz), 29.7 (br), 28.6, 26.8 (*pseudo* t, $^3J_{CP}$ = 5.8 Hz), 26.6 (*pseudo* t, $^3J_{CP}$ = 5.1 Hz), 26.2, 17.4, 14.7, 14.4, 11.9, 10.4 (br), 2.5 ppm; **^{31}P{^{1}H} NMR** (202 MHz, $CDCl_3$) δ 12.7 (br), −143.6 (septet, $^1J_{PF}$ = 712.6 Hz) ppm; **^{11}B{^{1}H} NMR** (128 MHz, $CDCl_3$) δ −1.7 ppm; **IR** (neat): $\tilde{\nu}$ = 2959 (w), 2929 (w), 2854 (w), 1552 (s), 1448 (m), 1360 (m), 1320 (s), 1261 (m), 1173 (s), 1146 (s), 1112 (m), 1021 (w), 982 (m), 945 (s) cm^{-1}; **HRMS** (ESI^+) calcd for $C_{74}H_{108}B_2N_4P_2Cu_1$ $[M - C_2H_3N_1]^+$ requires *m*/*z* 1197.7598, found *m*/*z* 1197.7583 (1.3 ppm).

$[Ag(2a)_2(hfa)]$ (6a)

(1,5-Cyclooctadiene)(hexafluoroacetylacetonato)silver(I) (0.031 g, 0.074 mmol), and 8-(4-diphenylphosphine)phenyl-4,4-diphenyl-1,3,5,7-tetramethyl-2,6-diethyl-4-bora-3a,4a-diaza-*s*-indacene (0.100 g, 0.147 mmol) were added together to anhydrous dichloromethane (2 mL) in a darkened flask and stirred at room temperature under nitrogen for one hour. After removal of the solvent an orange solid was produced, which was washed with anhydrous hexane (3 × 5 mL). Yield 0.103 g (87%). A sample suitable for X-ray crystallographic analysis was obtained from chloroform–hexane. **^{1}H NMR** (500 MHz, $CDCl_3$) δ 7.63–7.55 (br d, $^3J_{HH}$ = 7.6 Hz, 4H), 7.52–7.45 (m, 12H), 7.43–7.37 (m, 20H), 7.29–7.24 (m, 8H), 7.23–7.18 (m, 4H), 5.70 (br, 1H), 2.40 (q, $^3J_{HH}$ = 7.8 Hz, 8H), 1.80 (s, 12H), 1.35 (s, 12H), 0.91 (t, $^3J_{HH}$ = 7.8 Hz, 12H) ppm; **^{13}C{^{1}H} NMR** (126 MHz, $CDCl_3$) δ 175.9 (d, J_{CP} = 30.7 Hz), 153.6, 150.5 (br), 139.9 (d, J_{CP} = 37.4 Hz), 134.9, 134.4 (d, J_{CP} = 6.7 Hz), 134.2, 133.9, 133.2, 132.8, 131.8, 131.6, 130.6, 130.5, 129.7, 129.1, 127.3, 125.6, 117.9 (q, $^1J_{CF}$ = 288.9 Hz), 86.7, 17.5, 14.8, 14.7, 12.2 ppm; **^{31}P{^{1}H} NMR** (202 MHz, $CDCl_3$) δ 10.2 (br) ppm; **^{11}B{^{1}H} NMR** (128 MHz, $CDCl_3$) δ −1.1 ppm; **^{19}F{^{1}H} NMR** (376 MHz, $CDCl_3$) δ −76.6 ppm; **IR** (neat): $\tilde{\nu}$ = 2966 (w), 2928 (w), 2870 (w), 1662 (m), 1520 (s), 1472 (m), 1434 (m), 1302 (m), 1171 (s), 972 (s) cm^{-1}; **HRMS** (ESI^+) calcd for $C_{94}H_{92}B_2N_4P_2Ag_1$ $[M - (C_5H_1F_6O_2)]^+$ requires *m*/*z* 1469.6068, found *m*/*z* 1469.6056 (1.6 ppm).

$[Ag(2b)_2(hfa)]$ (6b)

Prepared as for **6a** using 0.038 g (0.090 mmol) of (1,5-cyclooctadiene)(hexafluoroacetylacetonato)silver(I) and 0.100 g (0.180 mmol) of **2b**. Yield 0.103 g (80%). **^{1}H NMR** (400 MHz, $CDCl_3$) δ 7.44–7.23 (m, 28H), 5.90 (br, 1H), 2.44 (s, 12H), 2.29 (q, $^3J_{HH}$ = 7.3 Hz, 8H), 1.24 (s, 12H), 0.96 (t, $^3J_{HH}$ = 7.3 Hz, 12H), 0.27 (s, 12H) ppm; **^{13}C{^{1}H} NMR** (100 MHz, $CDCl_3$) δ 175.8 (d, J_{CP} = 30.8 Hz), 151.0, 139.6, 138.9, 134.2 (d, J_{CP} = 17.3 Hz), 133.7 (d, J_{CP} = 17.3 Hz), 133.3, 133.1, 132.7, 132.3 (d, J_{CP} = 23.0 Hz), 130.3, 129.5 (d, J_{CP} = 9.6 Hz), 129.0 (d, J_{CP} = 8.6 Hz), 128.7, 117.9 (q, $^1J_{CF}$ = 290.4 Hz), 88.9, 17.4, 14.6, 14.3, 11.9, 10.4 (br) ppm; **^{31}P{^{1}H} NMR** (162 MHz, $CDCl_3$) δ 6.6 (br) ppm; **^{11}B{^{1}H} NMR** (128 MHz, $CDCl_3$) δ −2.2 ppm; **^{19}F{^{1}H} NMR** (376 MHz, $CDCl_3$) δ −76.5 ppm; **IR** (neat): $\tilde{\nu}$ = 2963 (w), 2932 (w), 2871 (w), 1660 (m), 1552 (s), 1538 (s), 1436 (m), 1321 (s), 1253 (s), 1172 (s), 1143 (s), 945 (s), 800 (s) cm^{-1}; **HRMS** (ESI^+)

calcd for $C_{74}H_{84}B_2N_4P_2Ag_1$ [M − $(C_5H_1F_6O_2)$]$^+$ requires *m*/*z* 1217.5475, found *m*/*z* 1217.5443 (2.5 ppm).

[Ag(3a)$_2$(hfa)] (7a)

Prepared as for **6a** using 0.031 g (0.072 mmol) of (1,5-cyclooctadiene)(hexafluoroacetylacetonato)silver(I) and 0.100 g (0.144 mmol) of **3a**. Yield 0.110 g (90%). **^{1}H NMR** (500 MHz, $CDCl_3$) δ 7.80–7.90 (m, 4H), 7.42–7.38 (m, 12H), 7.25–7.17 (m, 12H), 5.71 (br, 1H), 2.37–2.01 (m, 8H), 2.19 (q, $^3J_{HH}$ = 7.3 Hz, 8H), 1.89–1.64 (m, 16H), 1.77 (s, 12H), 1.36–1.06 (m, 20H), 1.28 (s, 12H), 0.86 (t, $^3J_{HH}$ = 7.3 Hz, 12H) ppm; **^{13}C{^{1}H} NMR** (126 MHz, $CDCl_3$) δ 175.0 (d, J_{CP} = 30.2 Hz), 153.5, 150.4 (br), 139.5 (d, J_{CP} = 8.6 Hz), 135.4, 134.9, 133.9, 133.7, 133.2, 130.5, 129.1, 127.3, 125.6, 125.2, 118.2 (q, $^1J_{CF}$ = 290.8 Hz), 85.3, 32.6 (br), 29.4 (br), 28.2, 26.9 (br), 26.8 (br), 26.2, 17.4, 14.8, 14.7, 12.0 ppm; **^{31}P{^{1}H} NMR** (202 MHz, $CDCl_3$) δ 23.7 (d, $^1J_{107AgP}$ = 453 Hz), 23.7 (d, $^1J_{109AgP}$ = 517 Hz) ppm; **^{11}B{^{1}H} NMR** (128 MHz, $CDCl_3$) δ −1.0 ppm; **^{19}F{^{1}H} NMR** (376 MHz, $CDCl_3$) δ −76.7 ppm; **IR** (neat): $\tilde{\nu}$ = 2928 (w), 2853 (w), 1661 (s), 1548 (s), 1522 (s), 1474 (m), 1303 (m), 1250 (m), 1172 (s), 1133 (s), 973 (s) cm^{-1}; **HRMS** (ESI$^+$) calcd for $C_{94}H_{116}B_2N_4P_2Ag_1$ [M − $(C_5H_1F_6O_2)$]$^+$ requires *m*/*z* 1489.7979, found *m*/*z* 1489.7998 (1.3 ppm).

[Ag(3b)$_2$(hfa)] (7b)

Prepared as for **6a** using 0.037 g (0.090 mmol) of (1,5-cyclooctadiene)(hexafluoroacetylacetonato)silver(I) and 0.100 g (0.176 mmol) of **3b**. Yield 0.115 g (90%). A sample suitable for X-ray crystallographic analysis was obtained from chloroform–hexane. **^{1}H NMR** (500 MHz, $CDCl_3$) δ 7.77 (m, 4H), 7.37 (d, $^3J_{HH}$ = 7.8 Hz, 4H), 5.69 (br, 1H), 2.46 (s, 12H), 2.27 (q, $^3J_{HH}$ = 7.3 Hz, 8H), 2.22–1.69 (m, 20H), 1.34–0.88 (m, 24H), 1.22 (s, 12H), 0.96 (t, $^3J_{HH}$ = 7.3 Hz, 12H), 0.29 (s, 12H) ppm; **^{13}C{^{1}H} NMR** (126 MHz, $CDCl_3$) δ 174.9 (d, J_{CP} = 29.7 Hz), 150.9, 139.8, 139.2, 135.3, 134.5, 133.4, 132.8, 129.0, 128.2, 118.2 (q, $^1J_{CF}$ = 290.8 Hz), 85.2, 32.5 (br), 29.3 (br), 28.2, 27.0 (br), 26.9 (br), 26.2, 17.5, 14.7, 14.4, 11.7, 10.5 (br) ppm; **^{31}P{^{1}H} NMR** (202 MHz, $CDCl_3$) δ 23.9 (d, $^1J_{107AgP}$ = 453 Hz), 23.9 (d, $^1J_{109AgP}$ = 519 Hz) ppm; **^{11}B{^{1}H} NMR** (128 MHz, $CDCl_3$) δ −1.8 ppm; **^{19}F{^{1}H} NMR** (376 MHz, $CDCl_3$) δ −76.6 ppm; **IR** (neat): $\tilde{\nu}$ = 2930 (m), 2857 (w), 1663 (m), 1545 (s), 1525 (m), 1448 (m), 1361 (m), 1321 (s), 1251 (m), 1173 (s), 1146 (s), 944 (s) cm^{-1}; **HRMS** (ESI$^+$) calcd for $C_{74}H_{108}B_2N_4P_2Ag_1$ [M − $(C_5H_1F_6O_2)$]$^+$ requires *m*/*z* 1242.7329, found *m*/*z* 1242.7354 (2.0 ppm).

[AuCl(2a)] (8a)

Chloro(tetrahydrothiophene)gold(I) (0.047 g, 0.147 mmol) and 8-(4-diphenylphosphine)phenyl)-4,4-diphenyl-1,3,5,7-tetramethyl-2,6-diethyl-4-bora-3a,4a-diaza-*s*-indacene (0.100 g, 0.147 mmol) were added together to anhydrous dichloromethane (2 mL) and stirred under nitrogen for 1 hour. After removal of the solvent an orange/red solid was produced, which was washed with anhydrous hexane (3 × 5 mL) to remove the tetrahydrothiophene. The complex was purified using column chromatography on silica gel (chloroform–hexane 1 : 1, R_f = 0.4) to yield an orange solid (0.101 g, 75%). A sample suitable for X-ray crystallographic analysis was obtained from chloroform–hexane. **^{1}H NMR** (400 MHz, $CDCl_3$) δ 7.68–7.61 (m, 2H), 7.60–7.45 (m, 12H), 7.30–7.28 (m, 4H), 7.18–7.10 (m, 6H), 2.16 (q, $^3J_{HH}$ = 7.3 Hz, 4H), 1.69 (s, 6H), 1.26 (s, 6H), 0.82 (t, $^3J_{HH}$ = 7.3 Hz, 6H) ppm; **^{13}C{^{1}H} NMR** (100 MHz, $CDCl_3$) δ 153.7, 149.9 (br), 141.7, 138.2, 134.5, 134.3 (d, J_{CP} = 13.4 Hz), 134.0 (d, J_{CP} = 13.4 Hz), 133.7, 133.3, 132.1 (d, J_{CP} = 2.9 Hz), 130.2, 130.0 (d, J_{CP} = 11.5 Hz), 129.3 (d, J_{CP} = 11.5 Hz), 128.6, 127.9, 127.1, 125.5, 17.3, 14.7, 14.6, 12.2 ppm; **^{31}P{^{1}H} NMR** (202 MHz, $CDCl_3$) δ 33.2 ppm; **^{11}B{^{1}H} NMR** (128 MHz, $CDCl_3$) δ −1.1 ppm; **IR** (neat): $\tilde{\nu}$ = 2962 (w), 1544 (s), 1472 (m), 1435 (s), 1142 (m), 1101 (m), 972 (s) cm^{-1}; **HRMS** (ESI$^+$) calcd for $C_{47}H_{46}B_1N_2P_1Cl_1Au_1$ [M]$^+$ requires *m*/*z* 912.2960, found *m*/*z* 911.2989 (3.2 ppm).

[AuCl(2b)] (8b)

Prepared in the same manner as for **8a** using 0.058 g (0.180 mmol) of chloro(tetrahydrothiophene)gold(I) and 0.100 g (0.180 mmol) of **2b**. The complex was purified using column chromatography on silica gel (dichloromethane–hexane 2 : 1, R_f = 0.4). Yield 0.129 g (91%). **^{1}H NMR** (400 MHz, $CDCl_3$) δ 7.66–7.58 (m, 2H), 7.57–7.52 (m, 4H), 7.52–7.44 (m, 8H), 2.44 (s, 6H), 2.30 (q, $^3J_{HH}$ = 7.3 Hz, 4H), 1.28 (s, 6H), 0.99 (t, $^3J_{HH}$ = 7.3 Hz, 6H), 0.27 (s, 6H) ppm; **^{13}C{^{1}H} NMR** (100 MHz, $CDCl_3$) δ 151.2, 141.6, 137.9, 134.3 (d, J_{CP} = 13.4 Hz), 134.0 (d, J_{CP} = 13.4 Hz), 133.1, 132.9, 132.1 (d, J_{CP} = 1.9 Hz), 129.9 (d, J_{CP} = 12.4 Hz), 129.3 (d, J_{CP} = 11.5 Hz), 128.6, 128.5, 128.0, 17.4, 14.6, 14.3, 12.0, 10.3 (br) ppm; **^{31}P{^{1}H} NMR** (162 MHz, $CDCl_3$) δ 33.3 ppm; **^{11}B{^{1}H} NMR** (128 MHz, $CDCl_3$) δ −2.0 ppm; **IR** (neat): $\tilde{\nu}$ = 2962 (w), 2926 (w), 2866 (w), 1552 (s), 1436 (m), 1314 (m), 1170 (s), 1101(s), 946 (s) cm^{-1}; **HRMS** (AP$^+$) calcd for $C_{37}H_{43}B_1N_2P_1Cl_1Au_1$ [M + H]$^+$ requires *m*/*z* 788.2642, found *m*/*z* 788.2627 (1.9 ppm).

[AuCl(3a)] (9a)

Prepared in the same manner as for **8a** using 0.046 g (0.144 mmol) of chloro(tetrahydrothiophene)gold(I) and 0.100 g (0.144 mmol) of **3a**. The complex was purified using column chromatography on silica gel (dichloromethane–hexane 1 : 1, R_f = 0.5). Yield 0.116 g (87%). A sample suitable for X-ray crystallographic analysis was obtained from chloroform–diethyl ether. **^{1}H NMR** (500 MHz, $CDCl_3$) δ 7.89–7.78 (m, 2H), 7.52–7.49 (m, 2H), 7.37–7.30 (m, 4H), 7.25–7.16 (m, 6H), 2.32 (m, 2H), 2.21 (q, $^3J_{HH}$ = 7.3 Hz, 4H), 2.11–2.09 (m, 2H), 1.89–1.63 (m, 8H), 1.77 (s, 6H), 1.43–1.10 (m, 10H), 1.27 (s, 6H), 0.89 (t, $^3J_{HH}$ = 7.3 Hz, 6H) ppm; **^{13}C{^{1}H} NMR** (126 MHz, $CDCl_3$) δ 153.9, 150.3 (br), 141.3 (d, J_{CP} = 2.9 Hz), 138.5, 135.3 (d, J_{CP} = 11.6 Hz), 134.7, 133.9, 133.5, 130.4, 129.7 (d, J_{CP} = 10.6 Hz), 127.3, 125.7, 125.2, 33.5 (d, $^1J_{CP}$ = 34.7 Hz), 29.7 (d, $^2J_{CP}$ = 1.9 Hz), 28.4, 26.5 (d, $^3J_{CP}$ = 5.7 Hz), 26.4 (d, $^3J_{CP}$ = 2.9 Hz), 25.9, 17.4, 14.8, 14.7, 12.2 ppm; **^{31}P{^{1}H} NMR** (202 MHz, $CDCl_3$) δ 51.4 ppm; **^{11}B{^{1}H} NMR** (128 MHz, $CDCl_3$) δ −1.0 ppm; **IR** (neat): $\tilde{\nu}$ = 2926 (w), 2854 (w), 1545 (s), 1473 (m), 1304 (m), 1263 (m), 1172 (s), 1143 (m), 972 (s) cm^{-1}; **HRMS** (AP$^+$) calcd for $C_{47}H_{59}B_1N_2P_1Au_1Cl_1$ [M + H]$^+$ requires *m*/*z* 924.3897, found *m*/*z* 924.3904 (1.1 ppm).

Table 2 Crystallographic data

Compound	**2a**	**4a**	**4b**	**5a** (structure **A**)	**5a** (structure **B**)
Chemical formula	$C_{47}H_{46}BN_2P$	$C_{98}H_{102}B_2CuN_4O_2P_2$	$C_{76}H_{90}B_2CuN_4OP_2^+\cdot PF_6^-$	$C_{96}H_{119}B_2CuN_5P_2^+\cdot PF_6^-\cdot C_4H_{10}O\cdot 2CHCl_3$	$C_{94}H_{116}B_2CuN_4P_2^+\cdot PF_6^-\cdot 2CHCl_3$
Formula mass	680.6	1514.9	1367.6	1947.9	1832.7
Crystal system	Monoclinic	Monoclinic	Triclinic	Triclinic	Monoclinic
a/Å	29.596(7)	22.626(2)	10.7978(6)	11.2490(2)	13.7756(6)
b/Å	8.231(2)	10.2574(8)	12.4349(7)	17.1875(4)	10.2495(5)
c/Å	31.073(12)	20.8126(19)	28.2720(15)	26.6167(6)	33.6122(17)
α/°			80.643(4)	93.8881(19)	
β/°	102.186(2)	111.403(10)	86.405(4)	93.6056(17)	91.672(4)
γ/°			72.103(5)	92.9238(19)	
Unit cell volume/Å^3	7399(4)	4497.2(7)	3564.0(4)	5116.22(19)	4743.8(4)
Space group	$I2/a$	$P2/c$	$P\bar{1}$	$P\bar{1}$	$P2/c$
Z	8	2	2	2	2
μ/mm^{-1}	0.075	0.327	1.575	0.476	0.508
No. of reflections measured	28 804	32 492	21 401	83 501	30 847
No. of independent reflections	6727	7915	11 052	20 525	9235
R_{int}	0.0601	0.1080	0.0392	0.0496	0.0394
R (F, $F^2 > 2\sigma$)	0.0457	0.0803	0.0617	0.0728	0.0827
R_w (F^2, all data)	0.1133	0.2213	0.1729	0.2236	0.2228
Goodness of fit on F^2	1.065	1.033	1.035	1.023	1.072
Difference map extremes/e Å^{-3}	0.32, −0.27	0.39, −0.41	0.72, −0.38	1.69, −1.32	1.28, −0.64

Compound	**6a**	**7b**	**8a**	**9a**	**9b**
Chemical formula	$C_{99}H_{93}AgB_2F_6N_4O_2P_2$	$C_{79}H_{109}AgB_2F_6N_4O_2P_2$	$C_{47}H_{46}AuBClN_2P_2\cdot CHCl_3$	$C_{47}H_{58}AuBClN_2P\cdot 0.5C_4H_{10}O$	$C_{37}H_{54}AuBClN_2P\cdot CHCl_3$
Formula mass	1676.2	1452.1	1032.4	962.2	920.4
Crystal system	Monoclinic	Monoclinic	Orthorhombic	Triclinic	Monoclinic
a/Å	17.8281(6)	34.386(6)	9.5273(7)	8.9183(14)	18.2559(8)
b/Å	16.4975(4)	10.3299(19)	15.9516(10)	15.431(3)	9.4353(4)
c/Å	28.2893(12)	24.444(5)	28.6394(14)	17.126(3)	23.1349(10)
α/°				106.221(2)	
β/°	93.976(5)	107.786(2)		91.812(2)	93.337(4)
γ/°				97.007(2)	
Unit cell volume/Å^3	8300.4(5)	8268(3)	4352.5(5)	2240.8(7)	3978.2(3)
Space group	$I2/a$	$C2/c$	$P2_12_12_1$	$P\bar{1}$	$P2_1/c$
Z	4	4	4	2	4
μ/mm^{-1}	2.857	0.285	9.234	3.110	4.036
No. of reflections measured	13 509	35 858	11 804	23 163	40 350
No. of independent reflections	6411	9121	6623	10 658	9004
R_{int}	0.0417	0.1189	0.0477	0.0431	0.0409
R (F, $F^2 > 2\sigma$)	0.0476	0.0839	0.0544	0.0432	0.0307
R_w (F^2, all data)	0.1272	0.2293	0.1495	0.0964	0.0668
Goodness of fit on F^2	0.958	1.019	1.002	1.098	1.059
Difference map extremes/e Å^{-3}	0.59, −0.54	0.82, −0.85	3.13, −1.66	1.49, −1.09	1.35, −1.10

[AuCl(3b)] (9b)

Prepared in the same manner as for **8a** using 0.056 g (0.176 mmol) of chloro(tetrahydrothiophene)gold(I) and 0.100 g (0.176 mmol) of **3b**. The complex was purified using column chromatography on silica gel (dichloromethane–hexane 1 : 1, R_f = 0.4). Yield 0.121 g (86%). A sample suitable for X-ray crystallographic analysis was obtained from chloroform–pentane. **^{1}H NMR** (500 MHz, $CDCl_3$) δ 7.78 (m, 2H), 7.47 (m, 2H), 2.44 (s, 6H), 2.30 (q, $^3J_{HH}$ = 7.5 Hz, 4H), 2.09–1.70 (m, 10H), 1.39–0.85 (m, 12H), 1.21 (s, 6H), 0.98 (t, $^3J_{HH}$ = 7.5 Hz, 6H), 0.27 (s, 6H) ppm; **^{13}C{^{1}H} NMR** (126 MHz, $CDCl_3$) δ 151.3, 141.6 (d, J_{CP} = 2.8 Hz), 138.2, 135.4 (d, J_{CP} = 11.6 Hz), 133.1 (d, J_{CP} = 17.3 Hz), 129.6 (d, J_{CP} = 10.6 Hz), 128.6, 125.4, 125.0, 33.5 (d, $^1J_{CP}$ = 34.7 Hz), 29.6 (d, $^2J_{CP}$ = 2.9 Hz), 28.4, 26.5 (d, $^3J_{CP}$ = 6.7 Hz), 26.4 (d, $^3J_{CP}$ = 3.9 Hz), 25.9, 17.5, 14.8, 14.4, 11.9, 10.5 (br) ppm; **^{31}P{^{1}H} NMR** (202 MHz, $CDCl_3$) δ 51.6 ppm; **^{11}B{^{1}H} NMR** (128 MHz, $CDCl_3$) δ −2.1 ppm; **IR** (neat): $\tilde{\nu}$ = 2924 (m), 2851 (w), 1552 (s), 1447 (m), 1359 (m), 1324 (s), 1263 (w), 1173 (s), 1147 (s), 945 (s) cm^{-1}; **HRMS** (EI$^+$) calcd for $C_{37}H_{53}B_1N_2P_1Au_1Cl_1$ $[M - H]^+$ requires m/z 798.3424, found m/z 798.3426 (0.2 ppm).

X-ray crystallography

Data were collected at 150 K (120 K for **2a**) on an Agilent Technologies Gemini A Ultra diffractometer with MoKα (λ = 0.71073 Å, for **4a**, **5a** structures **A** and **B**, and **9b**) or CuKα (λ = 1.54178 Å, for **4b**, **6a**, and **8a**) radiation,[41] and on a Crystal Logics diffractometer equipped with a Rigaku Saturn 724+ detector at beamline I19 of Diamond Light Source using a synchrotron X-ray wavelength of 0.6889 Å (for **2a**, **7b**, and **9a**).[42] Selected crystallographic information is given in Table 2. Absorption corrections were based on multiple and symmetry-equivalent data; the structures were solved by direct and heavy-atom methods, and refined on all unique F^2 values with appropriate constraints and/or restraints in each case, particularly for the treatment of disordered structural components.[43] Unidentified solvent and/or counter-ion in the structure of the complex obtained from the attempted recrystallization of **4a** was treated by the Squeeze procedure of PLATON;[44] H atoms could not be observed in difference maps for this relatively low-precision structure, so it is not clear whether the complex is a neutral Cu(II) complex with two ethoxide ligands or a cationic Cu(I) complex with two ethanol ligands and a highly disordered small anion, though the latter is more likely from the observed tetrahedral geometry. Further discussion and evidence from spectroscopic data is provided in the ESI.† CCDC references: 987389 (**2a**), 987388 (**4a**), 987387 (**4b**), 987386 (**5a A**), 987385 (**5a B**), 987390 (**6a**), 987384 (**7b**), 987391 (**8a**), 987383 (**9a**) and 987382 (**9b**).

Acknowledgements

We thank Newcastle University for funding (L. H. D.) and the EPSRC for a Career Acceleration Fellowship (L. J. H.), an equipment grant (W. C.), their National Mass Spectrometry Service Centre, Swansea, UK, and the Newcastle-operated synchrotron component of their National Crystallography Service. We also thank Diamond Light Source for access to synchrotron facilities. We are grateful to Johnson Matthey for the loan of certain precious metal salts.

Notes and references

1 (*a*) F. L. Thorp-Greenwood, *Organometallics*, 2012, **31**, 5686–5692; (*b*) H. Kobayashi, M. Ogawa, R. Alford, P. L. Choyke and Y. Urano, *Chem. Rev.*, 2009, **110**, 2620.

2 S.-G. Lim and S. A. Blum, *Organometallics*, 2009, **28**, 4643.

3 K. A. Stephenson, S. R. Banerjee, T. Besanger, O. O. Sogbein, M. K. Levadala, N. McFarlane, J. A. Lemon, D. R. Boreham, K. P. Maresca, J. D. Brennan, J. W. Babich, J. Zubieta and J. F. Valliant, *J. Am. Chem. Soc.*, 2004, **126**, 8598.

4 (*a*) N. Inoue, Y. Suzuki, K. Yokoyama and I. Karube, *Biosci., Biotechnol., Biochem.*, 2009, **73**, 1215; (*b*) N. Soh, O. Sakawaki, K. Makihara, Y. Odo, T. Fukaminato, T. Kawai, M. Irie and T. Imato, *Bioorg. Med. Chem.*, 2005, **13**, 1131; (*c*) M. Onoda, S. Uchiyama, A. Endo, H. Tokuyama, T. Santa and K. Imai, *Org. Lett.*, 2003, **5**, 1459; (*d*) K. Akasaka, T. Suzuki, H. Ohrui and H. Meguro, *Anal. Lett.*, 1987, **20**, 731; (*e*) J. Pan, J. A. Downing, J. L. McHale and M. Xian, *Mol. Biosyst.*, 2009, **5**, 918; (*f*) T. Hatakeyama, S. Hashimoto and M. Nakamura, *Org. Lett.*, 2011, **13**, 2130; (*g*) S. Cai, Y. Lu, S. He, F. Wei, L. Zhao and X. Zeng, *Chem. Commun.*, 2013, **49**, 822; (*h*) J. C. Vaughan, G. T. Dempsey, E. Sun and X. Zhuang, *J. Am. Chem. Soc.*, 2013, 135.

5 L. H. Davies, B. Stewart and L. J. Higham, Part (III) Air-stable, Fluorescent Primary Phosphines, in *Organometallic Chemistry*, ed. I. Fairlamb and J. Lynam, Royal Society of Chemistry, 2014, vol. 39, p. 51.

6 (*a*) A. Loudet and K. Burgess, *Chem. Rev.*, 2007, **107**, 4891; (*b*) G. Ulrich, R. Ziessel and A. Harriman, *Angew. Chem., Int. Ed.*, 2008, **47**, 1184.

7 (*a*) S. Berners-Price and P. Sadler, Phosphines and Metal Phosphine Complexes: Relationship of Chemistry to Anticancer and Other Biological Activity, in *Bioinorganic Chemistry: Structure & Bonding*, Springer, Germany, 1988, vol. 70, pp. 27–102; (*b*) C. F. Shaw, *Chem. Rev.*, 1999, **99**, 2589; (*c*) J.-Y. Maillard and P. Hartemann, *Crit. Rev. Microbiol.*, 2012, **37**, 373.

8 (*a*) S. Tian, F.-M. Siu, S. C. F. Kui, C.-N. Lok and C.-M. Che, *Chem. Commun.*, 2011, **47**, 9318; (*b*) S. J. Berners-Price, C. K. Mirabelli, R. K. Johnson, M. R. Mattern, F. L. McCabe, L. F. Faucette, C.-M. Sung, S.-M. Mong, P. J. Sadler and S. T. Crooke, *Cancer Res.*, 1986, **46**, 5486; (*c*) L. E. Wedlock, M. R. Kilburn, J. B. Cliff, L. Filgueira, M. Saunders and S. J. Berners-Price, *Metallomics*, 2011, **3**, 917.

9 (*a*) S. J. Berners-Price, R. K. Johnson, A. J. Giovenella, L. F. Faucette, C. K. Mirabelli and P. J. Sadler, *J. Inorg. Biochem.*, 1988, **33**, 285; (*b*) S. J. Berners-Price, D. C. Collier, M. A. Mazid, P. J. Sadler, R. E. Sue and D. Wilkie,

Met.-Based Drugs, 1995, **2**, 111; (*c*) S. J. Berners-Price, R. J. Bowen, P. J. Harvey, P. C. Healy and G. A. Koutsantonis, *J. Chem. Soc., Dalton Trans.*, 1998, 1743.

10 (*a*) S. J. Berners-Price, R. K. Johnson, C. K. Mirabelli, L. F. Faucette, F. L. McCabe and P. J. Sadler, *Inorg. Chem.*, 1987, **26**, 3383; (*b*) R. J. Bowen, M. Navarro, A.-M. J. Shearwood, P. C. Healy, B. W. Skelton, A. Filipovska and S. J. Berners-Price, *Dalton Trans.*, 2009, 10861; (*c*) C. Marzano, V. Gandin, M. Pellei, D. Colavito, G. Papini, G. G. Lobbia, E. Del Giudice, M. Porchia, F. Tisato and C. Santini, *J. Med. Chem.*, 2008, **51**, 798; (*d*) J. S. Lewis, J. Zweit and P. J. Blower, *Polyhedron*, 1998, **17**, 513; (*e*) S. Alidori, G. Gioia Lobbia, G. Papini, M. Pellei, M. Porchia, F. Refosco, F. Tisato, J. Lewis and C. Santini, *J. Biol. Inorg. Chem.*, 2008, **13**, 307.

11 B. Sutton, *Gold Bull.*, 1986, **19**, 15.

12 C. K. Mirabelli, R. K. Johnson, C. M. Sung, L. Faucette, K. Muirhead and S. T. Crooke, *Cancer Res.*, 1985, **45**, 32.

13 W. A. Volkert, W. F. Goeckeler, G. J. Ehrhardt and A. R. Ketring, *J. Nucl. Med.*, 1991, **32**, 174.

14 (*a*) P. J. Blower, J. S. Lewis and J. Zweit, *Nucl. Med. Biol.*, 1996, **23**, 957; (*b*) P. McQuade, D. W. McCarthy and M. J. Welch, Metal Radionuclides for PET Imaging, in *Positron Emission Tomography*, ed. D. L. Bailey, D. W. Townsend, P. E. Valk and M. N. Maisey, Springer, London, 2005, pp. 237–250.

15 L. H. Davies, B. Stewart, R. W. Harrington, W. Clegg and L. J. Higham, *Angew. Chem., Int. Ed.*, 2012, **51**, 4921.

16 B. J. Dunne and A. G. Orpen, *Acta Crystallogr., Sect. C: Cryst. Struct. Commun.*, 1991, **47**, 345.

17 A. M. Leiva, L. Rivera and B. Loeb, *Polyhedron*, 1991, **10**, 347.

18 Z. Mao, H.-Y. Chao, Z. Hui, C.-M. Che, W.-F. Fu, K.-K. Cheung and N. Zhu, *Chem. – Eur. J.*, 2003, **9**, 2885.

19 J. V. Hanna, R. D. Hart, P. C. Healy, B. W. Skelton and A. H. White, *J. Chem. Soc., Dalton Trans.*, 1998, 2321.

20 J. Díez, S. Falagán, P. Gamasa and J. Gimeno, *Polyhedron*, 1988, **7**, 37.

21 (*a*) F. H. Allen, *Acta Crystallogr., Sect. B: Struct. Sci.*, 2002, **58**, 380; (*b*) C. R. Groom and F. H. Allen, *Angew. Chem., Int. Ed.*, 2014, **53**, 662.

22 (*a*) S. Noro, T. Akutagawa and T. Nakamura, *Chem. Commun.*, 2010, **46**, 4619; (*b*) W. G. Haanstra, W. L. Driessen, R. A. G. de Graaff, G. C. Sebregts, J. Suriano, J. Reedijk, U. Turpeinen, R. Hamalainen and J. S. Wood, *Inorg. Chim. Acta*, 1991, **189**, 243; (*c*) C.-C. Su and C.-B. Li, *Polyhedron*, 1994, **13**, 825; (*d*) P. Gentschev, N. Moller and B. Krebs, *Inorg. Chim. Acta*, 2000, **300**, 442; (*e*) F. Bachechi, A. Burini, M. Fontani, R. Galassi, A. Macchioni, B. R. Pietroni, P. Zanello and C. Zuccaccia, *Inorg. Chim. Acta*, 2001, **323**, 45; (*f*) P. Comba, C. L. de Laorden and H. Pritzkow, *Helv. Chim. Acta*, 2005, **88**, 647; (*g*) A. Prescimone, J. Sanchez-Benitez, K. K. Kamenev, S. A. Moggach, J. E. Warren, A. R. Lennie, M. Murrie, S. Parsons and E. K. Brechin, *Dalton Trans.*, 2009, **39**, 113; (*h*) B. Korybut-Daszkiewicz, J. Taraszewska, K. Zieba, A. Makal and K. Wozniak, *Eur. J. Inorg. Chem.*, 2004, 3335; (*i*) A. J. Blake, P. Hubberstey, W.-S. Li, C. E. Russell, B. J. Smith and L. D. Wraith, *J. Chem. Soc., Dalton Trans.*, 1998, 647; (*j*) E. Coronado, J. R. Galan-Mascaros, P. Gavina, C. Marti-Gastaldo, F. M. Romero and S. Tatay, *Inorg. Chem.*, 2008, **47**, 5197; (*k*) C. D. Ene, C. Maxim, F. Tuna and M. Andruh, *Inorg. Chim. Acta*, 2009, **362**, 1660.

23 R. J. Restivo, A. Costin, G. Ferguson and A. J. Carty, *Can. J. Chem.*, 1975, **53**, 1949.

24 J. Green, E. Sinn, S. Woodward and R. Butcher, *Polyhedron*, 1993, **12**, 991.

25 (*a*) A. Baiada, F. H. Jardine and R. D. Willett, *Inorg. Chem.*, 1990, **29**, 3042; (*b*) A. Baiada, F. H. Jardine and R. D. Willett, *Inorg. Chem.*, 1990, **29**, 4805.

26 (*a*) I. J. Colquhoun and W. McFarlane, *J. Chem. Soc., Chem. Commun.*, 1980, 145; (*b*) E. L. Muetterties and C. W. Alegranti, *J. Am. Chem. Soc.*, 1972, **94**, 6386.

27 L. J. Baker, G. A. Bowmaker, D. Camp, Effendy, P. C. Healy, H. Schmidbaur, O. Steigelmann and A. H. White, *Inorg. Chem.*, 1992, **31**, 3656.

28 Z. Yuan, N. H. Dryden, J. J. Vittal and R. J. Puddephatt, *Chem. Mater.*, 1995, **7**, 1696.

29 D. A. Edwards, R. M. Harker, M. F. Mahon and K. C. Molloy, *J. Mater. Chem.*, 1999, **9**, 1771.

30 Z. Yuan, N. H. Dryden, J. J. Vittal and R. J. Puddephatt, *Can. J. Chem.*, 1994, **72**, 1605.

31 (*a*) R. G. Goel and P. Pilon, *Inorg. Chem.*, 1978, **17**, 2876; (*b*) E. C. Alyea, S. A. Dias and S. Stevens, *Inorg. Chim. Acta*, 1980, **44**, L203.

32 (*a*) M. Altaf and H. Stoeckli-Evans, *Inorg. Chim. Acta*, 2010, **363**, 2567; (*b*) M. Altaf and H. Stoeckli-Evans, *Polyhedron*, 2010, **29**, 701.

33 (*a*) D. Gibson, B. F. G. Johnson and J. Lewis, *J. Chem. Soc. A*, 1970, 367; (*b*) W. Partenheimer and E. H. Johnson, *Inorg. Chem.*, 1973, **12**, 1274.

34 (*a*) N. C. Baenziger, W. E. Bennett and D. M. Soborofe, *Acta Crystallogr., Sect. B: Struct. Crystallogr. Cryst. Chem.*, 1976, **32**, 962; (*b*) J. A. Muir, S. I. Cuadrado and M. M. Muir, *Acta Crystallogr., Sect. C: Cryst. Struct. Commun.*, 1991, **47**, 1072; (*c*) J. A. Muir, M. M. Muir, L. B. Pulgar, P. G. Jones and G. M. Sheldrick, *Acta Crystallogr., Sect. C: Cryst. Struct. Commun.*, 1985, **41**, 1174.

35 (*a*) A. Kaloudi-Chantzea, N. Karakostas, C. P. Raptopoulou, V. Psycharis, E. Saridakis, J. Griebel, R. Hermann and G. Pistolis, *J. Am. Chem. Soc.*, 2010, **132**, 16327; (*b*) M.-H. Ha-Thi, M. Penhoat, D. Drouin, M. Blanchard-Desce, V. Michelet and I. Leray, *Chem. – Eur. J.*, 2008, **14**, 5941; (*c*) W. Wu, J. Zhao, J. Sun, L. Huang and X. Yi, *J. Mater. Chem. C*, 2013, **1**, 705.

36 (*a*) A. Coskun and E. U. Akkaya, *J. Am. Chem. Soc.*, 2005, **127**, 10464; (*b*) Y. Gabe, Y. Urano, K. Kikuchi, H. Kojima and T. Nagano, *J. Am. Chem. Soc.*, 2004, **126**, 3357.

37 (*a*) T. S. Teets, D. V. Partyka, A. J. Esswein, J. B. Updegraff, M. Zeller, A. D. Hunter and T. G. Gray, *Inorg. Chem.*, 2007,

46, 6218; (*b*) T. S. Teets, J. B. Updegraff, A. J. Esswein and T. G. Gray, *Inorg. Chem.*, 2009, **48**, 8134.
38 R. Uson, A. Laguna, M. Laguna, D. A. Briggs, H. H. Murray and P. Frackler, *Inorg. Synth.*, 1989, **26**, 85.
39 J. Schraml, M. Čapka and V. Blechta, *Magn. Reson. Chem.*, 1992, **30**, 544.
40 *Spartan 10*, Wavefunction Inc., Irvine, California, 2011.
41 *CrysAlisPro*, Agilent Technologies Ltd., Oxford, 2008–2013.
42 *CrystalClear*, Rigaku Corporation, Tokyo, Japan, 2008–2013; *APEX2*, Bruker AXS Inc., Madison, Wisconsin, 2008–2013.
43 *SHELXTL*, Bruker AXS Inc., Madison, Wisconsin, 2008–2013; G. M. Sheldrick, *SHELXL-2013*, University of Göttingen, Germany, 2013.
44 A. L. Spek, *Acta Crystallogr., Sect. D: Biol. Crystallogr.*, 2009, **65**, 148.